

This discussion paper is/has been under review for the journal *Atmospheric Chemistry and Physics (ACP)*. Please refer to the corresponding final paper in *ACP* if available.

**Particulate
ammonium modelling
for North America
using AURAMS**

P. A. Makar et al.

Modelling the impacts of ammonia emissions reductions on North American air quality

P. A. Makar¹, M. D. Moran¹, Q. Zheng¹, S. Cousineau², M. Sassi², A. Duhamel², M. Besner², D. Davignon², L.-P. Crevier², and V. S. Bouchet²

¹Air Quality Research Division, Science and Technology Branch, Environment Canada, Toronto, Ontario, Canada

²Air Quality Model Applications Section, Meteorological Service of Canada, Environment Canada, Montreal, Quebec, Canada

Received: 19 December 2008 – Accepted: 28 January 2009 – Published: 2 March 2009

Correspondence to: P. A. Makar (paul.makar@ec.gc.ca)

Published by Copernicus Publications on behalf of the European Geosciences Union.

Title Page

Abstract

Introduction

Conclusions

References

Tables

Figures

⏪

⏩

◀

▶

Back

Close

Full Screen / Esc

Printer-friendly Version

Interactive Discussion

Abstract

A unified regional air-quality modelling system (AURAMS) was used to investigate the effects of reductions in ammonia emissions on regional air quality, with a focus on particulate-matter formation. Three simulations of one-year duration were performed for a North American domain: (1) a base-case simulation using 2002 Canadian and US national emissions inventories augmented by a more detailed Canadian emissions inventory for agricultural ammonia; (2) a 30% North-American-wide reduction in agricultural ammonia emissions; and (3) a 50% reduction in Canadian beef-cattle ammonia emissions. The simulations show that a 30% continent-wide reduction in agricultural ammonia emissions lead to reductions in median hourly $PM_{2.5}$ mass of $<1 \mu g m^{-3}$ on an annual basis. The atmospheric response to these emission reductions displays marked seasonal variations, and on even shorter time scales the impacts of the emissions reductions are highly episodic: 95-percentile hourly $PM_{2.5}$ mass decreases can be up to a factor of six larger than the median values.

A key finding of the modelling work is the linkage between gas and aqueous chemistry and transport; reductions in ammonia emissions affect gaseous ammonia concentrations close to the emissions site, but substantial impacts on particulate matter and atmospheric deposition often occur at considerable distances downwind, with particle nitrate being the main vector of ammonia/ μm transport. Ammonia emissions reductions therefore have trans-boundary and possibly trans-oceanic consequences downwind. Calculations of critical-load exceedances for sensitive ecosystems in Canada suggest that ammonia emission reductions will have a minimal impact on current ecosystem acidification within Canada, but may have a substantial impact on future ecosystem acidification. The 50% Canadian beef-cattle ammonia emissions reduction scenario was used to examine model sensitivity to uncertainties in the new Canadian agricultural ammonia emissions inventory, and the simulation results suggest that further work is needed to improve the emissions inventory for this particular sector.

ACPD

9, 5371–5422, 2009

Particulate ammonium modelling for North America using AURAMS

P. A. Makar et al.

Title Page

Abstract

Introduction

Conclusions

References

Tables

Figures

⏪

⏩

◀

▶

Back

Close

Full Screen / Esc

Printer-friendly Version

Interactive Discussion

1 Introduction

The chemistry describing the interactions of atmospheric ammonia (NH_3) with other atmospheric constituents has been well established through field and laboratory studies. While very high concentrations of ammonia gas are known to have health impacts (e.g., Stigl, 1994), its role in the creation of airborne particulate matter (PM) at lower concentrations is of interest due to the known effects of fine particulate matter on human health (cf. Schwarze et al., 2006).

The creation of airborne PM from ammonia is dependant on the presence of other precursor gases, primarily directly-emitted sulphur dioxide and nitrogen oxides (SO_2 and NO_x ; Seinfeld and Pandis, 1998). SO_2 may oxidize via gas-phase (Stockwell and Calvert, 1983) and/or aqueous-phase (Coste and Courtier, 1936; Junge and Ryan, 1958; Hermann et al., 2000, 2005) reactions, creating sulphuric acid gas or sulphuric acid ions in cloud or rain water, respectively. The vapour pressure of sulphuric acid gas is sufficiently low that almost all of the gas created will partition to the particle phase, either through condensation on existing particles or nucleation of new particles. Sulphuric acid created in cloud and/or rainwater may be transferred to the particle phase upon droplet evaporation.

Ammonia affects aqueous-phase chemistry through the provision of a weak base; the hydrogen ion concentration will be inversely proportional to the ammonia partial pressure. Reductions in the hydrogen ion concentration due to excess ammonia will allow a greater aqueous uptake of SO_2 in cloud water in the form of the bisulphite ion (HSO_3^-). The latter may be oxidized by hydrogen peroxide, ozone, organic peroxides, or catalytic oxygen reactions to bisulphate and sulphate ions, the ionic equilibrium products of sulphuric acid dissociation (Hermann et al., 2000, 2005). H_2O_2 is believed to be the dominant aqueous-phase oxidant of HSO_3^- , but the strongly pH-dependent oxidation by O_3 becomes more important as pH increases or when H_2O_2 has been depleted (e.g., Fung et al., 1991). The relative contribution of these two oxidants to aqueous-phase sulphate formation is therefore influenced by NH_3 levels. An additional process

Particulate ammonium modelling for North America using AURAMS

P. A. Makar et al.

Title Page

Abstract

Introduction

Conclusions

References

Tables

Figures

⏪

⏩

◀

▶

Back

Close

Full Screen / Esc

Printer-friendly Version

Interactive Discussion

of importance for ammonia chemistry is the formation of gaseous nitric acid (HNO_3) through well-known “ NO_x termination” reactions (Seinfeld and Pandis, 1998); HNO_3 may in turn participate in aqueous reactions with the ammonium ion, or in particle-phase chemistry.

Laboratory studies and related thermodynamics of high-concentration particle ammonium chemistry are well established (cf. D’Ans, 1913), and observations of ammonium, sulphate, and nitrate in PM have appeared in the literature over the past sixty years (cf. Robbins and Cadle, 1958; Fenn et al., 1963; Spurny and Heard, 1969; Heard and Wiffen, 1969; Gordon and Bryan, 1973; Anlauf et al., 1978; Brosset, 1978; Stelson et al., 1979; Tanner, 1983). The partitioning between different phases, including gases, may be predicted using fundamental thermodynamics theory (cf. Kusik and Meissner, 1978) in box models (e.g., Ansari and Pandis, 1999) or regional models such as AURAMS (Makar et al., 2003; Gong et al., 2006).

The concept of ammonia limitation may be introduced, in order to better understand the aqueous and particulate chemistry of ammonia. Small perturbations in the ammonia concentration will have a significant effect on particle concentrations while the ammonia remains insufficient to charge-balance the available anions. Ammonia emissions changes for this situation may therefore have a significant impact on particle concentrations, and ammonia availability limits the inorganic fine-mode particle mass. When the ammonia is available in excess, perturbations to the ammonia concentration will have little impact on particulate matter mass; an anion-limited environment. Here, the atmosphere is said to be “ammonia-limited” when there are insufficient moles of total ammonium (ammonia gas + all ammonium as aqueous phase or particulate ions, or crystalline ammonium salts) to charge balance the total number of moles of sulphate. A broader definition of ammonia-limited environments includes a requirement for charge balancing with nitrate and other anions; the use of sulphate restricts the definition to strongly ammonia-limited environments, where changes in ammonia emissions would be expected to result in a significant change in particulate matter mass.

Comprehensive Eulerian regional models are useful tools for studying the poten-

Particulate ammonium modelling for North America using AURAMS

P. A. Makar et al.

Title Page

Abstract

Introduction

Conclusions

References

Tables

Figures

⏪

⏩

◀

▶

Back

Close

Full Screen / Esc

Printer-friendly Version

Interactive Discussion

**Particulate
ammonium modelling
for North America
using AURAMS**P. A. Makar et al.

[Title Page](#)[Abstract](#)[Introduction](#)[Conclusions](#)[References](#)[Tables](#)[Figures](#)[⏪](#)[⏩](#)[◀](#)[▶](#)[Back](#)[Close](#)[Full Screen / Esc](#)[Printer-friendly Version](#)[Interactive Discussion](#)

tial impacts of ammonia emissions on atmospheric particle formation and deposition to sensitive ecosystems. The first generation of these models were designed to predict the gas-phase concentrations of acidifying gases, ozone, other reactive gases, and wet and dry deposition of atmospheric acidic species (e.g., Chang et al., 1987; Venkatram and Karamchandani, 1988). Later work extended these models to include size-distributed PM (Binkowski and Shankar, 1995). Further developments within the last decade included the introduction of more detailed inorganic and organic particulate chemistry, and the introduction of size-resolved and speciated PM (e.g., Binkowski and Roselle, 2003; Gong et al., 2006). More recently, these models have begun to be used to investigate the role of ammonia and other nitrogen compounds in atmospheric chemistry and deposition (Mathur and Dennis, 2003; Ying and Kleeman, 2006; Phillips et al., 2006; Luo et al., 2007; Quan and Zhang, 2008; Wang et al., 2008). A recent extension of deposition modelling to assess environmental impacts is the calculation of exceedances of acid-deposition critical loads (defined below) in order to estimate the impact of deposition on sensitive ecosystems (Fowler et al., 1998; Dentener et al., 2006; Spranger et al., 2008; Fenn et al., 2008).

Various emission control strategies have been suggested in recent years to reduce ambient PM levels in North America, including controls on ammonia emissions. In this paper, we describe the application of a comprehensive regional air-quality model to predict the likely effects of reductions in North American emissions of agricultural ammonia on the mass and composition of atmospheric PM and on the amount of acid deposition to sensitive ecosystems. Three one-year simulations, a 2002 base case and two hypothetical NH_3 emission scenarios, have been run and analyzed. The next section describes the study methodology. Section 3 summarizes a performance evaluation for the 2002 base case, and Sect. 4 analyzes the results of the two emission scenarios. Finally, conclusions and recommendations for further study are provided in Sect. 5.

2 Methodology

2.1 Modelling system description

AURAMS (A Unified Regional Air-quality Modelling System) consists of three main components: (a) a prognostic meteorological model, GEM (Global Environmental Multi-scale model: Côté et al., 1998); (b) an emissions processing system, SMOKE (Sparse Matrix Operator Kernel Emissions: Houyoux et al., 2000; CEP, 2003); and (c) an off-line regional chemical transport model, the AURAMS Chemical Transport Model (CTM: Gong et al., 2006).

The GEM meteorological model is an integrated weather forecasting and data assimilation system that was designed to meet Canada's operational needs for both short- and medium-range weather forecasts. For the 2002 simulation, GEM version 3.2.0 with physics version 4.2 was run on the variable-resolution global horizontal grid centred on North America.

Files of gridded hourly emission fields (including ammonia) for input by the AURAMS CTM were prepared using version 2.2 of the SMOKE emissions processing system for four major emissions streams: on-road mobile sources; area and offroad-mobile sources, minor point sources; and major point sources. Emitted (i.e., "primary") PM from these sources is speciated within the AURAMS CTM based on speciation profiles for each emissions stream, and these profiles include some primary particulate ammonium. The mass of ammonium emitted as primary particulate ammonium, however, is much smaller than the mass of gaseous ammonia emissions, and most particulate ammonium ($p\text{-NH}_4$) is created through chemical reactions (i.e., "secondary" sources). A simulation of this partitioning between ammonia gas and $p\text{-NH}_4$ takes place within the chemical modules of the AURAMS CTM.

The multi-pollutant, regional AURAMS CTM was developed as a tool to study the formation of ozone, PM, and acid deposition in a single "unified" framework. The PM size distribution in this study was represented using 12 size bins ranging from 0.01 to 41 μm in Stokes diameter and nine chemical components: sulphate ($p\text{-SO}_4$); nitrate

Particulate ammonium modelling for North America using AURAMS

P. A. Makar et al.

Title Page

Abstract

Introduction

Conclusions

References

Tables

Figures

⏪

⏩

◀

▶

Back

Close

Full Screen / Esc

Printer-friendly Version

Interactive Discussion



**Particulate
ammonium modelling
for North America
using AURAMS**

P. A. Makar et al.

[Title Page](#)[Abstract](#)[Introduction](#)[Conclusions](#)[References](#)[Tables](#)[Figures](#)[⏪](#)[⏩](#)[◀](#)[▶](#)[Back](#)[Close](#)[Full Screen / Esc](#)[Printer-friendly Version](#)[Interactive Discussion](#)

(p -NO₃); ammonium (p -NH₄); elemental carbon (EC); primary organic matter (POM); secondary organic matter (SOM); crustal material (CM); sea salt; and particle-bound water. PM is assumed to be internally mixed in each size bin. Process representations in version 1.3.1b of the AURAMS CTM include emissions from surface and from elevated sources, horizontal and vertical advection, vertical diffusion, gas-phase, aqueous-phase, and inorganic heterogeneous chemistry, secondary organic particle formation, dry and wet deposition, and particle nucleation, condensation, coagulation, sedimentation, and activation (Gong et al., 2006). Up to 157 model species (gases and speciated particle size bins) may be selected as model output, although summary measures such as PM_{2.5} bulk mass are compared to observations here.

AURAMS inorganic particle components are reported as the mass of sulphate, nitrate, and ammonium within each particle bin size, but within the model, the inorganic heterogeneous chemistry module (Makar et al., 2003) performs equilibrium calculations to determine the relative amounts of mass of ammonium sulphate ((NH₄)₂SO₄(s)), ammonium bisulphate (NH₄HSO₄(s)), letovicite ((NH₄)₃H(SO₄)₂(s)), ammonium nitrate (NH₄NO₃(s)), and the ammonium (NH₄⁺(aq)), sulphate (SO₄²⁻(aq)), bisulphate (HSO₄⁻(aq)), and nitrate ions (NO₃⁻(aq)). The reported sulphate mass (p -SO₄) is thus the sum of sulphate mass from all particle components containing sulphate, with similar sums for the nitrate and ammonium mass.

The representation of dry deposition of ammonia gas within AURAMS follows Zhang et al. (2002); deposition is parameterized as a weighted combination of the deposition properties of ozone and SO₂. Dry deposition of p -NH₄ is a function of particle size (Zhang et al., 2001). It should be noted that AURAMS does not include the possible “co-deposition” of SO₂(g) and NH₃(g). Some researchers have found evidence of enhanced deposition of both gases when both are present at the same site (e.g., Neiryneck et al., 2005; Van Hove et al., 1989; Adema et al., 1986). Others have found no effect (Erisman et al., 1994a, b), and Sutton et al. (1994) found enhanced emissions of ammonia gas from natural surfaces when ambient NH₃ is present. More observational work on co-deposition is needed before parameterizations for this process may

be reliably included in air-quality models.

The time-invariant, vertically-varying chemical lateral boundary conditions used in AURAMS CTM are taken from a variety of sources. Latitudinally-dependent O₃ boundary conditions were taken from a monthly-varying climatology (Logan, 1998). CO boundary conditions were derived from vertical profiles in Wang et al. (1999), with a simple latitudinal dependence of concentration peaking at 45 N, in rough accord with satellite observations. Speciated particulate boundary conditions (including p-NH₄) were based on data collected at an elevated site on Whistler Mountain on the Canadian west coast (MacDonald et al., 2006), with a similar simple latitude dependence assumed as for CO. Seasonally-varying profiles of the concentrations of other reactive gases (including NH₃) were taken from a set of “clean” chemical boundary conditions from simulations of the ADOM regional acid-deposition model (Scire et al., 1986; Fung et al., 1991).

2.2 Model domain, grid discretization, and simulation period

The GEM horizontal grid consisted of 353×415 grid points on a rotated latitude-longitude map projection with grid spacing of approximately 24 km (0.22°) on the 270×353 uniform regional “core” grid. In the vertical 28 hybrid-coordinate levels reached from the Earth’s surface to 10 hPa, with layer thickness increasing monotonically with height. A time step of 450 s was used.

The uniform horizontal grid used for the AURAMS CTM was 150×106 in size and spanned the North American continent on a secant polar-stereographic projection true at 60° N, with a horizontal grid spacing of 42 km (see Fig. 1). Twenty-eight terrain-following vertical levels stretched telescopically from the Earth’s surface to 29 km, with the first three levels at 0, 13.9, and 55 m a.g.l. An advective time step of 900 s was used, and AURAMS-predicted fields were output hourly. Both GEM and the AURAMS CTM were run for the 13-month period from 1 December 2001 to 31 December 2002, where the first month was treated as a spin-up period for the AURAMS CTM. GEM was run from analyzed fields for 396 overlapping 30-h segments starting 24 h apart,

Particulate ammonium modelling for North America using AURAMS

P. A. Makar et al.

Title Page

Abstract

Introduction

Conclusions

References

Tables

Figures

⏪

⏩

◀

▶

Back

Close

Full Screen / Esc

Printer-friendly Version

Interactive Discussion



where the first six hours of each segment were treated as a “spin-up” period and were discarded. The remaining 24 h of consecutive simulations were then “stitched” together to create a complete set of meteorological fields with a 900 s timestep for input to the AURAMS CTM. The CTM itself was run in three segments, with a one-month spin-up for each segment, allowing an entire year’s simulation to be run in parallel on multiple processors in order to reduce simulation “wall-clock” time.

2.3 Description of emissions scenarios

The hourly gridded anthropogenic emissions files used in this study were generated using SMOKE v2.2 (<http://www.smoke-model.org/index.cfm>) based on the 2002 Canadian (obtained from Environment Canada), 2002 US (obtained from US EPA), and 1999 Mexican (obtained from US EPA) national criteria-air-contaminant inventories. Biogenic emissions are calculated on-line in the AURAMS CTM using BEIS version 3.09 (Biogenic Emissions Inventory System: CEP, 2003). The following three 2002 annual emissions scenarios were considered.

1. Base Case: Canadian 2002 ammonia emissions from the default national inventory were replaced with those resulting from a more detailed inventory constructed as part of the National Agri-Environmental Standards Initiative (NAESI), a multi-year study which included the collection of Canada-specific emission factors and activity levels (Ayres et al., 2009; Bittman et al., 2009). The scenario using these combined emissions inventories will be referred to hereafter as the “Base Case”. The kilotonne emissions of ammonia gas for the base case on a seasonal basis are shown in Fig. 2.
2. 30% agricultural NH₃ emissions reduction, Canada and US: The base case’s agricultural emissions of NH₃ (including emissions from animal husbandry and from fertilizer application) were reduced by a factor of 30% at all times and locations in both countries.

Particulate ammonium modelling for North America using AURAMS

P. A. Makar et al.

Title Page

Abstract

Introduction

Conclusions

References

Tables

Figures

⏪

⏩

◀

▶

Back

Close

Full Screen / Esc

Printer-friendly Version

Interactive Discussion

3. 50% Canadian beef cattle NH₃ emissions reduction: a 50% reduction in Canadian emissions from this single sub-sector was implemented in order to test model sensitivity to sub-sector-specific inventory uncertainty estimates of a factor of two.

2.4 Metrics and Diagnostic Fields for Scenario Analysis

5 The key species of interest in this study are the model-predicted values of gaseous ammonia, SO₂, and nitric acid, as well as the total PM_{2.5} mass and PM_{2.5} inorganic composition. Differences between base case and scenario (i.e., base case value – scenario value) for these species show the impacts of the change in emissions of NH₃, with positive values indicating decreases in the mass or concentration arising from the
10 reduction in NH₃ emissions.

In order to explain the chemistry associated with the base case, and the chemical reasons for the changes associated with the emissions-reduction scenarios, four chemical metrics based on the ambient air concentrations of several species have been employed. The metrics and their interpretation are given in Table 1.

15 A number of diagnostic deposition fields were also calculated to help quantify the impacts of changes in NH₃ emissions on atmospheric chemistry and deposition. The derived deposition fields include the total amount of sulphur deposited per season (sum of wet deposition and dry deposition of all species containing sulphur), the total amount of nitrate deposited, the total amount of ammonium deposited, and the total amount
20 of nitrogen deposited. Subcomponents of these diagnostics will also be occasionally referenced (e.g., the amount of wet-deposited sulphate+SO₂ as a fraction of the total sulphur deposition).

Another important set of diagnostic outputs calculated for the AURAMS analysis were exceedances of annual critical loads in Canada. The “critical load” of an ecosystem refers to its ability to buffer acidifying precipitation. The underlying concept is that
25 an ecosystem will have the ability to absorb a certain amount of acidifying sulphur and nitrogen compounds, including NH₃ and *p*-NH₄, without damage to the ecosystem itself. If the rate of deposition of these compounds exceeds the rate at which the

Particulate ammonium modelling for North America using AURAMS

P. A. Makar et al.

Title Page

Abstract

Introduction

Conclusions

References

Tables

Figures

⏪

⏩

◀

▶

Back

Close

Full Screen / Esc

Printer-friendly Version

Interactive Discussion



ecosystem can naturally absorb the compounds, however, ecosystem damage begins to occur. The maximum amount of acidifying mass that an ecosystem can absorb per unit area in a year is known as its annual critical load, and any additional deposited mass that exceeds that amount is known as an annual critical load exceedance (e.g., Jeffries et al., 1999; Hall et al., 2001; Jeffries and Ouimet, 2004; McNulty et al., 2007). Critical loads depend on local bedrock type, soil type and thickness, and other factors.

Sulphur deposition is essentially entirely acidifying, but nitrogen has a large biological activity, and may be stored in various catchment compartments within an ecosystem (Jeffries and Ouimet, 2004). Eventually, though, an ecosystem may reach a steady state with regard to nitrogen deposition (termed “nitrogen saturation”), after which all further nitrogen deposition is acidifying. Sulphur critical-load exceedance thus describes conditions where immediate ecosystem damage will occur, whereas sulphur + nitrogen critical-load exceedance describes conditions where ecosystem damage will once the ecosystem’s ability to absorb nitrogen is overwhelmed. Critical-load exceedances for sulphur + nitrogen thus describe a worst-case scenario, in which all of the deposited nitrogen is assumed to be acidifying. At the current time, Canadian ecosystems are not nitrogen-saturated (Jeffries and Ouimet, 2004); exceedances of sulphur + nitrogen critical loads thus indicate the potential for future ecosystem damage, as opposed to current ecosystem damage.

3 Model performance evaluation for the base case

The statistics used here for evaluation of the base case for the AURAMS simulations were used previously as part of an extensive AURAMS performance evaluation against measurements for the 2002 calendar year (Moran et al., 2007, 2008). The statistical measures used for the comparison are shown in Table 2. Measurements from 15 different Canadian and US air-chemistry and precipitation-chemistry networks and sub-networks were used to evaluate the base-case fields.

A number of steps were followed in preparing the measurements for comparison

Particulate ammonium modelling for North America using AURAMS

P. A. Makar et al.

Title Page

Abstract

Introduction

Conclusions

References

Tables

Figures

⏪

⏩

◀

▶

Back

Close

Full Screen / Esc

Printer-friendly Version

Interactive Discussion

with model predictions. For example, units were adjusted as required to a common set of units (e.g., concentrations at ambient conditions to concentrations at STP). Data records from individual stations were screened for temporal completeness, and if they passed, then measurements were combined to create seasonal and annual values for the station. In locations where more than one station was located in an AURAMS CTM grid cell, the measurements were averaged. Even so, measurements from multiple air-chemistry networks are quite heterogeneous, since individual networks have different goals and objectives, choose different types of sampling locations, employ different sampling instruments, techniques, and protocols, and measure different species (e.g., Eder and Yu, 2006). For example, individual networks have very different sampling periods, ranging from hourly to weekly, and sampling intervals that vary from hourly, to 1 day in 6, to weekly. Combining measurements from different network does provide the benefits of increased sample size, spatial coverage, and spatial density, but the price paid is greater variability within the combined measurement data set.

The resulting annual statistics for ambient concentrations of the key species related to $p\text{-NH}_4$ formation and removal, with the exception of NH_3 , for which routine measurements are not available, are shown in Table 3, and those relating to wet deposition are shown in Table 4.

These comparisons to observations show that, on an annual basis, AURAMS under-predicted the base-case $\text{PM}_{2.5}$ bulk mass by 31%, the $\text{PM}_{2.5}$ inorganic species concentrations by 18% to 19%, the concentration of inorganic ions in precipitation by 11% to 33%, and the wet deposition of inorganic ions by 6% to 24% (negative normalized mean biases). The implication of the comparison is that the model estimates for the base case for the $\text{PM}_{2.5}$ components and precipitation species are likely to be lower than the ambient atmosphere, and that model-predicted critical-load exceedances, described below, are likely to be underestimates. The impact of the model bias on the scenarios is harder to quantify. The usual assumption that is made is that the bias will be linear, so that the scenarios will have the same normalized biases as the base case. The impacts of ammonia emission reductions on the real atmosphere are therefore ex-

Particulate ammonium modelling for North America using AURAMS

P. A. Makar et al.

Title Page

Abstract

Introduction

Conclusions

References

Tables

Figures



Back

Close

Full Screen / Esc

Printer-friendly Version

Interactive Discussion



pected to be similar in relative magnitude and sign as simulated here but may vary in the absolute sense.

4 Scenario analysis

4.1 Analysis of the base case

5 One means of identifying NH_3 -limited environments is to calculate the total (ammonia + ammonium) to sulphate mole ratio (cf. Table 1). Seasonal fields of this metric for the 2002 base case are shown in Fig. 3. Yellow to red areas in this figure have a large excess of NH_3 and are not strongly NH_3 -limited: significant reductions in NH_3 emissions would be required to reach NH_3 -limited conditions. These areas tend to correspond to areas of high NH_3 emissions (cf. Fig. 2). Green to blue regions, on the other hand, are NH_3 -limited, with more acidic conditions. Reductions in NH_3 emissions in these areas would have an immediate impact on ambient $\text{PM}_{2.5}$ levels. Pronounced seasonal and local variations can also be seen; summer and winter have the largest extent of NH_3 -limited regions.

15 One implication of the above analysis is that the regions that may benefit from NH_3 reductions will not necessarily be the regions that have the highest NH_3 emissions. For example, the region of greatest NH_3 saturation in Fig. 3 is centered on the US states of Minnesota, South Dakota, Nebraska, and Iowa – this also corresponds to the region of greatest NH_3 emissions. Reductions in NH_3 in this region are unlikely to significantly impact PM concentrations, due to the locally NH_3 -saturated chemistry. However, further to the east and downwind from this source region are the NH_3 -limited regions of the Great Lakes, the Ohio River Valley, and the Appalachian mountains. Depending on the extent to which NH_3 is transported, PM reductions are likely to occur downwind. The impact of NH_3 reductions will therefore be a combination of local chemistry and transport from higher-emission NH_3 -saturated regions to lower-emission NH_3 -limited regions.

Particulate ammonium modelling for North America using AURAMS

P. A. Makar et al.

Title Page

Abstract

Introduction

Conclusions

References

Tables

Figures

⏪

⏩

◀

▶

Back

Close

Full Screen / Esc

Printer-friendly Version

Interactive Discussion



4.2 Analysis of continental agricultural NH₃ emission reduction scenario

In this scenario, NH₃ emissions from agricultural sources were decreased uniformly by 30% in both Canada and the United States. In the following figures, the difference between base-case and scenario concentration fields will be displayed [(base case) – (scenario)], and the same difference formats will be used for the metrics. Positive values in the difference plots thus indicate decreases in the scenario concentrations relative to the base case; negative values indicate increases in the scenario concentrations relative to the base case. It is also important to note that seasonal average differences are being displayed unless noted otherwise; within each season, shorter duration events will occur with larger (and smaller) impacts than those depicted here.

4.2.1 NH₃ concentrations

The greatest decreases in seasonal NH₃ concentrations (Fig. 4) are closely matched with the locations of the main NH₃ emissions regions (Fig. 2). The effect of reductions in NH₃ emissions on NH₃ gas concentrations is therefore primarily local; most of the NH₃ is removed close to the source (either through deposition or conversion to PM).

The influence of seasonal variations in the NH₃ emissions can also be seen in Fig. 4. Agricultural emissions in North America are highest in the spring and lowest in the winter (e.g., Gilliland et al., 2006). As a consequence, the predicted change in concentration of NH₃ gas in the winter is lower than in the other seasons. For example, the decrease in ammonia concentrations in the high emissions region of Southern Minnesota in the summer is on the order of 2.5 ppbv, while the wintertime value in the same region is on the order of 0.5 ppbv.

4.2.2 PM_{2.5} concentrations

The impact of the NH₃ emissions reductions on average seasonal PM_{2.5} mass is shown in Fig. 5. Seasonally-averaged PM_{2.5} changes resulting from a 30% reduction in NH₃

Title Page

Abstract

Introduction

Conclusions

References

Tables

Figures

⏪

⏩

◀

▶

Back

Close

Full Screen / Esc

Printer-friendly Version

Interactive Discussion

**Particulate
ammonium modelling
for North America
using AURAMS**

P. A. Makar et al.

[Title Page](#)[Abstract](#)[Introduction](#)[Conclusions](#)[References](#)[Tables](#)[Figures](#)[⏪](#)[⏩](#)[◀](#)[▶](#)[Back](#)[Close](#)[Full Screen / Esc](#)[Printer-friendly Version](#)[Interactive Discussion](#)

emissions range from an increase of 0.07 to a decrease of $3.99 \mu\text{g m}^{-3}$. The greatest overall reductions in mass occur in spring and summer and occur in specific regions. The largest of these regions is centered over the Ohio River valley and Southern Ontario; most of the Eastern US and Southern Ontario and Quebec experience reductions in $\text{PM}_{2.5}$. Another region with reductions greater than $1 \mu\text{g m}^{-3}$ occurs in the US eastern seaboard corridor. Significantly, these regions do not coincide with the regions of largest NH_3 emission reductions (cf. Fig. 4). The San Joaquin valley of central California also shows seasonal average $\text{PM}_{2.5}$ reductions greater than $0.5 \mu\text{g m}^{-3}$ and locally as large as $2 \mu\text{g m}^{-3}$. The Vancouver to Seattle region has $\text{PM}_{2.5}$ reductions up to $1.5 \mu\text{g m}^{-3}$ in the summer; this effect is highly seasonal however, with a reduction of only $0.25 \mu\text{g m}^{-3}$ in the winter and intermediate reductions in the transition seasons. The Alberta-Saskatchewan area of Western Canada has smaller reductions in $\text{PM}_{2.5}$, on the order of 0.25 to $0.5 \mu\text{g m}^{-3}$, with the greatest reductions in the spring and fall.

The episodic nature of the changes in $\text{PM}_{2.5}$ mass resulting from ammonia emissions reductions has been examined by constructing annual frequency distributions of hourly mass difference and hourly percent mass difference between the base case and the 30%-reduction scenario. Hourly model values of the changes in $\text{PM}_{2.5}$ were first extracted for those model grid cells containing the CAPMoN and CASTNET monitoring stations shown in Fig. 6 and were then used to construct annual frequency distributions of hourly mass change (Fig. 7) and percent mass change (Fig. 8). In both Figs. 7 and 8, the sites are arranged roughly from the west of the continent on the left to the east of the continent on the right, and positive values indicate reductions relative to the base case. Both figures show that median hourly $\text{PM}_{2.5}$ reductions are usually less than $1 \mu\text{g m}^{-3}$, or on the order of 5% of the $\text{PM}_{2.5}$ mass at any given location, while the reductions during episodes (95 percentiles) may be considerably higher. For the Canadian sites (CAPMoN), the largest median mass reductions (Fig. 7a) are at Abbotsford Airport ($0.55 \mu\text{g m}^{-3}$) located in an agricultural area to the east of Vancouver, British Columbia, and Simcoe, Ontario, located in an agricultural area to the east of the De-

troit/Windsor conurbation ($0.50 \mu\text{g m}^{-3}$). The median values at all sites are much lower than the 95-percentile limits (e.g., Abbotsford Airport, 95 percentile value of $3.3 \mu\text{g m}^{-3}$; Simcoe, $3.2 \mu\text{g m}^{-3}$). Median percent reductions (Fig. 7b) are more centered in the frequency distributions, although the upper ends of the range are still considerably higher than the medians (e.g., Abbotsford Airport median and 95-percentile values of 3.8% and 17%; Simcoe 8.5% and 23%, respectively). A similar pattern may be observed at US sites (CASTNET), with median and 95 mass percentile values in Indiana and Ohio reaching 0.69 and $3.1 \mu\text{g m}^{-3}$, and 0.63 and $3.2 \mu\text{g m}^{-3}$, respectively, and corresponding percent reduction median and 95-percentile values of 8% and 22%, and 7.8% and 22%, respectively. The mass reduction distributions (Figs. 7a, 8a) suggest that the impact of ammonia controls on $\text{PM}_{2.5}$ mass will be episodic, with mass reductions during periods of elevated $\text{PM}_{2.5}$ levels being as much as 4 to 6 times greater than the median mass reduction. The percent mass reduction distributions (Figs. 7b, 8b) show that median percent mass decreases of 0 to 8% are predicted at the network locations in both countries, with 95-percentile values of up to 22%. However, Figs. 7 and 8 also show that NH_3 emission decreases can also lead to lower-magnitude episodic increases of $\text{PM}_{2.5}$ mass.

4.2.3 $\text{PM}_{2.5}$ chemistry

The manner in which the reductions in NH_3 emissions create the $\text{PM}_{2.5}$ mass reductions described above can be examined by considering the changes in the metrics of Table 1.

The predicted change in particle neutralization ratio resulting from a 30% reduction in NH_3 emissions relative to the base case is shown in Fig. 9. Positive regions indicate areas where the neutralization ratio has decreased (i.e., the particles have become more acidic) compared to the base case, and negative regions indicate areas where the neutralization ratio has increased (i.e., the particles have become less acidic). The main NH_3 emitting regions in the US midwest display relatively little change in particle

**Particulate
ammonium modelling
for North America
using AURAMS**

P. A. Makar et al.

Title Page

Abstract

Introduction

Conclusions

References

Tables

Figures

⏪

⏩

◀

▶

Back

Close

Full Screen / Esc

Printer-friendly Version

Interactive Discussion

charge balance; these regions are NH_3 -saturated, so there is little impact on particle charge balance in spite of the predicted concurrent decreases in ambient NH_3 concentrations (cf. Fig. 4). Substantial decreases in the particle neutralization ratio (i.e., increases in particle acidity and changes in particle composition) do occur downwind and on the fringes of the NH_3 emissions regions.

The predicted change in the total ammonium to sulphate ratio resulting from the 30% change in NH_3 emissions is shown in Fig. 10. The total ammonium to sulphate ratio describes the chemical regime, and Fig. 10 shows that the reduction in emitted NH_3 has resulted in a more acidic chemical regime over the NH_3 source regions, with relatively little change outside of those source regions. Figures 9 and 10 suggest that the composition of particles formed over the NH_3 source regions will change. For example, given the minor change in neutralization ratio in Southern Minnesota (Fig. 9), the drop in total ammonium to sulphate in these regions (Fig. 10) suggests that the particles may have more acidic components (ammonium bisulphate, etc.) over the source regions. That is, these two figures taken together suggest that particle nitrate is the dominant means of transport of NH_3 from the source regions to regions downwind; the mass of particle sulphate in the NH_3 source regions is invariant, and the lack of change in the neutralization ratio there shows that reductions in particle ammonium are being accompanied by reductions in particle nitrate. The downwind impact of the NH_3 emissions is therefore due in part to particle ammonium nitrate transport.

A strong seasonal variation in changes to chemical regime can also be seen in Fig. 10, particularly over the Canadian Prairies. Spring and fall have the greatest increase in particle regime acidity, while summer and winter have smaller changes.

The change in the mass fraction of NH_3 (i.e., $[\text{NH}_3(\text{g})] \{ [\text{NH}_3(\text{g})] + [\text{PM}_{2.5}-\text{NH}_4] \}$ on a mass basis) is shown in Fig. 11. The differences are positive over most of the domain and over all seasons, showing that a greater proportion of the remaining (ammonia + ammonium) mass resides in the particle phase instead of the gas phase following a reduction in NH_3 emissions. The effect is strongest in the summer and weakest in the winter. The figure suggests that reductions in NH_3 gas emissions will result in a

Particulate ammonium modelling for North America using AURAMS

P. A. Makar et al.

Title Page

Abstract

Introduction

Conclusions

References

Tables

Figures

⏪

⏩

◀

▶

Back

Close

Full Screen / Esc

Printer-friendly Version

Interactive Discussion

nonlinear reduction in NH_3 gas concentrations due to chemistry: a shift in chemical regime will reduce the relative amount of NH_3 that remains in the gas-phase.

The ratio of the sum of $\text{PM}_{2.5}$ nitrate and ammonium mass to total $\text{PM}_{2.5}$ mass is shown in Fig. 12. This figure shows that the relative amount of $\text{PM}_{2.5}$ composed of these NH_3 -sensitive species has decreased in the 30% reduction scenario. The figure is also of interest in that it confirms ammonium nitrate as the means of long-range transport of NH_3 mass. Comparing the summer (upper left) panels of Figs. 4, 5 and 12, it can be seen that:

1. The largest ammonia source region is located in Southern Minnesota and Northern Iowa (Fig. 4), while the largest particle mass reductions occur further to the east, north of the Ohio River (Fig. 5).
2. The region of greatest particle ammonium and nitrate reduction (Fig. 12) occurs over the state of Illinois i.e., between the ammonia source region and the region of greatest particle mass reduction.

The change in the fraction of directly NH_3 -sensitive particle mass has a strong seasonal variation, with the greatest impact in the winter (lower left panel, Fig. 12). This is consistent with the strong dependence of particle nitrate formation on temperature, with colder temperatures resulting in a greater proportion of ammonia and nitric acid gas being converted to particle ammonium nitrate, ammonium, and nitrate ions.

4.2.4 Total deposition

AURAMS calculates the wet and dry deposition of various species to the Earth's surface as $\text{moles m}^{-2} \text{h}^{-1}$. The hourly wet and dry deposition fields have been added together and summed to seasonal mass totals (kg/ha/season) for the following analysis. As before, scenario values are then subtracted from the base case to determine the impact of the reduced NH_3 emissions.

**Particulate
ammonium modelling
for North America
using AURAMS**

P. A. Makar et al.

Title Page

Abstract

Introduction

Conclusions

References

Tables

Figures

⏪

⏩

◀

▶

Back

Close

Full Screen / Esc

Printer-friendly Version

Interactive Discussion

**Particulate
ammonium modelling
for North America
using AURAMS**

P. A. Makar et al.

[Title Page](#)[Abstract](#)[Introduction](#)[Conclusions](#)[References](#)[Tables](#)[Figures](#)[⏪](#)[⏩](#)[◀](#)[▶](#)[Back](#)[Close](#)[Full Screen / Esc](#)[Printer-friendly Version](#)[Interactive Discussion](#)

The predicted change in total deposition of all forms of sulphur ($\text{SO}_2 + \text{H}_2\text{SO}_4 + p\text{-SO}_4$ dry deposition and wet deposition) is depicted in Fig. 13. The 30% reduction in the emissions of NH_3 has resulted in decreases in sulphur total deposition (red) in many regions in both Canada and the US. Increases in sulphur deposition are also present, in the colder seasons (SE US, Atlantic provinces). It should be noted that these predicted changes to the sulphur deposition associated with ammonia emissions reductions, while significant, are relatively small in magnitude relative to the total sulphur deposited: on the order of 1% of the total sulphur total deposition.

The predicted changes in sulphur total deposition are the result of the following NH_3 emissions-reduction-induced changes in the state of atmospheric sulphur:

1. A reduction in NH_3 reduces the capacity of cloud water and rain to absorb SO_2 , via the net equilibrium: $\text{NH}_3(\text{g}) + \text{SO}_2(\text{g}) + \text{H}_2\text{O} \rightleftharpoons \text{NH}_4^+(\text{aq}) + \text{HSO}_3^-(\text{aq})$.

The concentration of the ammonium ion decreases, hence less $\text{SO}_2(\text{g})$ can enter the aqueous phase as $\text{HSO}_3^-(\text{aq})$ in the absence of the buffering provided by NH_3 . The reduction of the sulphur content in cloud water and rain results in less sulphur being removed by wet deposition.

1. A corollary to (1) is that less sulphur is removed in precipitation. The sulphur, which remains in the form of $\text{SO}_2(\text{g})$, will therefore be transported longer distances due to decreased rainout/washout. The increases in sulphur deposition that takes place in the colder seasons in Fig. 13 (eastern seaboard of US, Atlantic Ocean) results from the transport and subsequent deposition of SO_2 to greater downwind distances.
2. Another corollary to (1) is that reductions in NH_3 emissions will reduce the amount of ammonium ion in the cloud droplets and water, and hence will reduce the amount of nitrate taken up in cloud water and rain, and thus the amount of nitrate removed by wet deposition. Total nitrogen deposition therefore decreases due to decreases in both reduced and oxidized nitrogen deposition, as discussed below.

Particulate ammonium modelling for North America using AURAMS

P. A. Makar et al.

[Title Page](#)[Abstract](#)[Introduction](#)[Conclusions](#)[References](#)[Tables](#)[Figures](#)[⏪](#)[⏩](#)[◀](#)[▶](#)[Back](#)[Close](#)[Full Screen / Esc](#)[Printer-friendly Version](#)[Interactive Discussion](#)

3. Reductions in NH_3 emissions may also cause a reduction in the size of ambient particles, since less NH_3 leads to less $p\text{-NH}_4$ and $p\text{-NO}_3$ in the particle phase, hence smaller particles, which have a smaller deposition velocity.

The change in total deposition of all phases of nitrogen related to ammonia chemistry (sum of $\{\text{NH}_4^+(\text{aq})+\text{NH}_3(\text{g})+\text{PM}_{2.5}\text{NH}_4+\text{NO}_3^-(\text{aq})+\text{HNO}_3(\text{g})+\text{PM}_{2.5}\text{NO}_3\}$) is shown in Fig. 14. The reduction in NH_3 emissions by 30% has resulted in substantial reductions in deposited nitrogen (similar in magnitude to the total deposited nitrogen in many locations). The greatest spatial extent of nitrogen deposition reduction occurs in the spring (lower right panel), when NH_3 emissions are highest, and the smallest change occurs in the winter (lower left panel), when NH_3 emissions are lowest. The location of the largest reductions in nitrogen deposition occurs over the NH_3 emitting areas (compare Figs. 4 and 14. Less than 10% of the total change in deposited nitrogen is associated with the various forms of nitrate, and is instead dominated by the ammonium components (not shown). The change in total ammonia/um deposition is itself dominated by $p\text{-NH}_4$ wet deposition (approximately 5/6 of the total) and NH_3 dry deposition (remaining 1/6), with changes to $p\text{-NH}_4$ dry deposition being relatively insignificant for the nitrogen budget.

The main results of the deposition analysis for a 30% reduction in agricultural NH_3 emissions are thus:

1. Sulphur deposition close to the sources of sulphur decreases slightly, due to a reduction in $\text{SO}_2(\text{g})$ uptake in clouds and possibly to a decrease in particle sulphate deposition with decreasing particle size. Sulphur deposition further downwind of the sources may increase as a consequence, depending on the season.
2. Nitrogen deposition decreases significantly, driven largely by decreases in $p\text{-NH}_4$ wet deposition but also by near-source decreases in $p\text{-NO}_3$ wet deposition.
3. Hydrogen ion wet deposition increases (not shown). The increase in hydrogen ion deposition is spatially matched with the decreases in nitrogen deposition and is greatest over the regions of NH_3 emissions.

4.2.5 Annual critical load exceedances for sensitive ecosystems

Annual critical-load exceedance fields for Canada were calculated for the base case and for the 30% emissions reduction scenario in two ways: for (a) sulphur (S) total deposition and for (b) sulphur+nitrogen (S+N) total deposition.

5 Annual critical-load exceedances for sulphur were not significantly changed between the base case and the 30% NH₃ emissions reduction scenario (annual critical-load exceedances did decrease for the NH₃ emissions reduction scenario, but significant reductions only occurred at two model gridpoints: not shown). This indicates that the impact of NH₃ emissions reductions on sulphur acidification of ecosystems is expected to be small, in accord with the relatively small changes in total sulphur deposition (Fig. 13).

10 Figure 15a shows the predicted S+N annual critical-load exceedances for the base case. Figure 15b shows the corresponding reductions in S+N annual critical-load exceedances in many parts of Canada that are predicted to result from a 30% reduction in agricultural NH₃ emissions. These substantial decreases in S+N annual critical-load exceedances are in contrast to the small decreases in S annual critical-load exceedances. The implication of this finding is that, if the ecosystem's ability to absorb nitrogen is compromised at these locations in the future, then the deposition of atmospheric nitrogen resulting from NH₃ emissions will contribute to a degradation of these ecosystems.

20 4.2.6 A conceptual model

The above analysis of AURAMS simulations may be used to provide a simple conceptual model to describe the effect of reductions in NH₃ emissions on atmospheric chemistry. The following diagram (Fig. 16) depicts the processes, on a hypothetical transect with NH₃ emissions on the left, a source of SO₂ and NO_x in the centre, and a receptor region downwind on the right. This is similar to the situation on the eastern half of the North American continent, with the US midwest NH₃ source on the left, the Ohio Valley and Great Lakes regions in the centre, and the Atlantic provinces and New

Particulate ammonium modelling for North America using AURAMS

P. A. Makar et al.

Title Page

Abstract

Introduction

Conclusions

References

Tables

Figures

⏪

⏩

◀

▶

Back

Close

Full Screen / Esc

Printer-friendly Version

Interactive Discussion

**Particulate
ammonium modelling
for North America
using AURAMS**

P. A. Makar et al.

[Title Page](#)[Abstract](#)[Introduction](#)[Conclusions](#)[References](#)[Tables](#)[Figures](#)[⏪](#)[⏩](#)[◀](#)[▶](#)[Back](#)[Close](#)[Full Screen / Esc](#)[Printer-friendly Version](#)[Interactive Discussion](#)

England states on the right. The prevailing wind blows from left to right in this diagram. The upper half of the diagram shows the system in the absence of NH_3 emission controls, the lower half the system including controls in NH_3 emissions. The size of the font for the different chemical variables is intended as a visual guide to the relative magnitude of those species, without (top) and with (bottom) NH_3 emissions controls.

In the absence of emissions controls (Fig. 16, top), excess NH_3 in the source region at left creates particle ammonium nitrate, in addition to particle ammonium sulphate. Winds blowing to the right then transport the particles and NH_3 gas. En route, the NH_3 gas is depleted due to wet and dry deposition, as are the particles by wet deposition. Nevertheless, significant amounts of particle ammonium and nitrate reach the SO_2 and NO_x emissions source region in the centre of the Figure. The addition of fresh SO_2 and nitric acid to the system cause the particles to locally become more acidic, with some transfer of the transported ammonium from particle nitrate to particle sulphate possible due to inorganic thermodynamics. With subsequent transport further downwind, the particles are deposited; relatively little SO_2 reaches far downwind locations due to NH_3 -enhanced aqueous-phase conversion to sulphate closer to the source regions.

With the presence of NH_3 controls (bottom), less ammonium nitrate is created in the Midwest source region, and hence less is available for transport. Smaller amounts of ammonium reach the central SO_2 and NO_x source region; this reduces the rate of further particle formation and allows more subsequent downwind transport and deposition of SO_2 . Downwind nitrogen and sulphur deposition is thus increased due to increased transport of these precursor species.

A neutral charge balance ratio (pink text in Fig. 16) is maintained over the NH_3 source region at the left regardless of the scenario; since this region remains NH_3 -saturated, reductions in $p\text{-NH}_4$ here are matched by reductions in $p\text{-NO}_3$ in the denominator. In the SO_2 and NO_x source region in the centre, however, the upwind reductions in NH_3 emissions result in a net decrease in charge balance and an increase in particle acidity that is then maintained during further downwind transport.

5 Uncertainty analysis of the 50% Canadian beef cattle emissions reduction scenario

The main intent of this scenario was to serve as an uncertainty benchmark for the previous scenario. The beef-cattle NH_3 emissions factors used in constructing the updated 2002 Canadian agricultural NH_3 emissions inventory were considered to be the most uncertain. Their uncertainty was estimated to be as high as a factor of two; the 50% reduction considered in this scenario thus represents the lower range of the uncertainty envelope.

The model response for $\text{PM}_{2.5}$ mass for this emissions scenario, relative to the base case, is shown below in Fig. 17. This figure uses the same colour scale as Fig. 5 to allow a direct comparison: the reduction of beef-cattle emissions by 50% has about the same impact in Alberta (in the area of concentrated beef-cattle operations) as the 30% overall reduction noted above. The only other region where a change is noticeable is in SW Ontario in the fall (upper right panel). There, the effect on $\text{PM}_{2.5}$ emissions is much smaller than that of the 30% overall emissions reduction scenario due to the smaller local relative contribution of beef-cattle NH_3 emissions to total NH_3 emissions.

One important conclusion from this analysis is that for Alberta, the range of uncertainty in model predictions associated with the beef-cattle emissions factors may be as large as the impacts from an across-the-board 30% reduction of NH_3 emissions. While the best available information was used to compile the new NH_3 emissions inventory, improvements in the beef-cattle subsector of the inventory are recommended for future work.

The other aspect to this sensitivity analysis is to demonstrate the extent to which sector-specific scenario simulations are possible with the updated 2002 NH_3 Canadian emissions inventory. An emissions reduction strategy may be “tailored” for the dominant emissions sources in a given region; very specific emissions reduction strategies may be tested in the future.

Particulate ammonium modelling for North America using AURAMS

P. A. Makar et al.

Title Page

Abstract

Introduction

Conclusions

References

Tables

Figures

⏪

⏩

◀

▶

Back

Close

Full Screen / Esc

Printer-friendly Version

Interactive Discussion

6 Conclusions and recommendations for future research

A unified regional air-quality modelling system (AURAMS) was used to investigate the effects of reductions in NH_3 emissions on regional air quality, especially PM. Three simulations of one-year duration were performed for a North American domain for different sets of NH_3 emissions. The simulation for a 30% continent-wide reduction in agricultural ammonia emissions predicted decreases in median hourly $\text{PM}_{2.5}$ mass of $\leq 1 \mu\text{g m}^{-3}$. However, the atmospheric response to these emission reductions has marked seasonal variations, and on even shorter time scales the impacts of the emissions reductions are highly episodic: for example, 95-percentile hourly $\text{PM}_{2.5}$ mass decreases may be a factor of six larger than the median values.

A key feature of the above simulations is the manner in which continental-scale long-range transport may play a role in defining the impacts of reductions in NH_3 emissions. The emissions reductions affect local NH_3 gas concentrations, but the largest impacts of these reductions may take place significantly downwind of the NH_3 emissions source in NH_3 -limited areas. The interaction between transport and chemistry is complex: NH_3 mass is transported from the source regions as aqueous and particle ammonium, and emissions of other particle precursors play a significant role in the subsequent chemistry. Reductions in NH_3 emissions result in a small but significant decrease in the amount of SO_2 gas converted to sulphate. Reductions in aqueous buffering capacity and decreases in particle size decrease local sulphur deposition in favour of SO_2 deposition further downwind; a by-product of the NH_3 emissions reduction is to increase the overall transport distance of emitted atmospheric sulphur. Ammonia emissions reductions result in a significant decrease in total ammonia deposition and a smaller decrease in nitrate deposition, in regions of high ammonia emissions.

The frequency-distribution figures of hourly model output for $\text{PM}_{2.5}$ mass show that the impact of NH_3 emissions reductions is highly episodic in nature. In both high and low resolution model runs, 95 percentile values of the differences between base case and scenarios are often much larger (up to a factor of 6) than the median differences

Particulate ammonium modelling for North America using AURAMS

P. A. Makar et al.

Title Page

Abstract

Introduction

Conclusions

References

Tables

Figures

⏪

⏩

◀

▶

Back

Close

Full Screen / Esc

Printer-friendly Version

Interactive Discussion

**Particulate
ammonium modelling
for North America
using AURAMS**

P. A. Makar et al.

[Title Page](#)[Abstract](#)[Introduction](#)[Conclusions](#)[References](#)[Tables](#)[Figures](#)[⏪](#)[⏩](#)[◀](#)[▶](#)[Back](#)[Close](#)[Full Screen / Esc](#)[Printer-friendly Version](#)[Interactive Discussion](#)

of the distribution. This is in accord with the known chemistry of $p\text{-NH}_4^+$ formation, specifically ammonium nitrate. Relatively small changes in local temperature, humidity, and precursor-gas concentrations can give rise to rapid particle formation and/or loss conditions (e.g., Yu et al., 2005). Decreases in NH_3 emissions may have a modest or low impact on $\text{PM}_{2.5}$ levels in median or average conditions, but a much larger impact when $\text{PM}_{2.5}$ levels are high.

Reductions in NH_3 emissions may result in decreases in acid deposition and in exceedance of S+N critical loads for sensitive Canadian ecosystems. The predicted small changes to sulphur deposition, on the other hand, have little impact on sulphur critical-load exceedances, implying that NH_3 emissions reductions at the current time will not reduce the sulphur acidification of sensitive ecosystems. However, if the ability of these ecosystems to absorb nitrogen becomes saturated, the role of NH_3 on the exceedance of critical loads does become substantial. Ammonia emissions reductions hence may eventually be required to reduce acidification of Canadian ecosystems.

The important linkages between transport and chemistry when NH_3 reductions are considered suggests that cross-border transport is an important factor with regards to predicting the outcomes of NH_3 reduction strategies. Ammonia and PM concentrations may be affected considerably downwind, and sulphur and nitrogen transport distances from sources of sulphur and nitrogen and associated deposition patterns are changed. Future scenario runs should focus on trans-boundary transport.

The beef-cattle emissions scenario shows that the uncertainty associated with the updated 2002 Canadian agricultural NH_3 emissions inventories for this source sub-sector is large. Future work on emissions inventories should attempt to reduce this uncertainty. This scenario also serves to show the potential for NH_3 emissions reduction scenarios that assess the impacts of agricultural-subsector-specific changes in emitting practices. Scenarios examining the impacts of NH_3 management practice changes should therefore be considered in future work.

A potentially significant source of uncertainty in all of the model results is the role of coarse-mode chemistry in the real atmosphere. Coarse-mode particle chemistry may

reduce the impact of ammonia emissions reductions by competing with the fine mode for the available nitric acid, as well as providing sites for condensation of nitric and sulphuric acid during intense dust storm events. Inclusion of coarse-mode chemistry is recommended for future model simulations of ammonia emission scenarios.

5 *Acknowledgements.* The authors are grateful for the financial assistance of the Canadian federal National Agri-Environmental Standards Initiative (NAESI) for carrying out this work.

References

Adema, E. H., Heeres, P., and Hulskotte: J. On the dry deposition of NH_3 , SO_2 , and NO_2 on wet surfaces in a small scale wind tunnel, in: Proceedings of the Seventh World Clean Air Congress, edited by: Hartman, H. F., Clean Air Society of Australia and New Zealand, 2, 1–8, 1986.

10 Anlauf, K. G., Lusic, M. A., and Wiebe, H. A.: Toronto Air Quality Study, Env. Canada report ARQA-60-78, 117 pp., 1978.

Ansari, A. S. and Pandis, S. N.: Prediction of multicomponent inorganic atmospheric aerosol behavior, *Atmos. Environ.*, 33, 745–757, 1999.

15 Ayres, J., Bittman, S., Girdhar, S., Sheppard, S., Niemi, D., Ratté, D., and Smith, P.: Chapter 5: Sources of Ammonia Emissions, The 2008 Canadian Atmospheric Assessment of Agricultural Ammonia, Environment Canada, Gatineau, QC, Canada, in press, 2009.

Binkowski, F. S. and Shankar, U.: The Regional Particulate Matter Model, 1. Model description and preliminary results, *J. Geophys. Res.*, 100, 26191–26209, 1995.

20 Binkowski, F. S. and Roselle, S. J.: Models-3 Community Multiscale Air Quality (CMAQ) model aerosol component 1. Model description, *J. Geophys. Res.-Atmos.*, 108, AAC 3-1–3-18, 2003.

25 Bittman, S., Ayres, J., Sheppard, S., and Girdhar, S.: Chapter 4: Emission Inventory Development, The 2008 Canadian Atmospheric Assessment of Agricultural Ammonia, Environment Canada, Gatineau, QC, Canada, in press, 2009.

Brosset, C.: Water-soluble sulphur compounds in aerosols, *Atmos. Environ.*, 12, 25–38, 1978.
CEP: Carolina Environmental Program: Sparse Matrix Operator Kernel Emission (SMOKE) modelling system, University of North Carolina, Carolina Environmental Programs, Chapel

Particulate ammonium modelling for North America using AURAMS

P. A. Makar et al.

Title Page

Abstract

Introduction

Conclusions

References

Tables

Figures

◀

▶

◀

▶

Back

Close

Full Screen / Esc

Printer-friendly Version

Interactive Discussion

**Particulate
ammonium modelling
for North America
using AURAMS**

P. A. Makar et al.

[Title Page](#)[Abstract](#)[Introduction](#)[Conclusions](#)[References](#)[Tables](#)[Figures](#)[⏪](#)[⏩](#)[◀](#)[▶](#)[Back](#)[Close](#)[Full Screen / Esc](#)[Printer-friendly Version](#)[Interactive Discussion](#)

Hill, NC, USA, online available at: <http://www.smoke-model.org/index.cfm>, last access: 23 February 2009, 2003.

Chang, J. S., Brost, R. A., Isaksen, I. S. A., Madronich, S., Middleton, P., Stockwell, W. R., and Walcek, C. J.: A three-dimensional Eulerian acid deposition model: Physical concepts and formulation, *J. Geophys. Res.*, 92, 14681–14700, 2003.

Coste, J. H. and Courtier, G. B.: Sulphuric acid as a disperse phase in town air, *T. Faraday Soc.*, 32, 1198–1202, 1936.

Côté, J., Gravel, S., Méthot, A., Patoine, A., Roch, M., and Staniforth, A.: The operational CMC-MRB Global Environmental Multiscale (GEM) model, Part 1: Design considerations and formulation, *Mon. Weather Rev.*, 126, 1373–1395, 1998.

D'Ans, J.: Zur Kenntnis der Suren Sulfate VII. Sulfate und Pyrosulfate des Natrium, Kalium und Ammonium. *Z. Allg. Anorg. On the knowledge of acidic sulphate VII. Acid sulphate and pyro-sulphate of sodium, potassium and ammonium*, *Journal for Inorganic and General Chemistry*, 80, 235–245, 1913.

Dentener, F., Drevet, J., Lamarque, J. F., Bey, I., Eickhout, B., Fiore, A. M., Hauglustaine, D., Horowitz, L. W., Krol, M., Kulshrestha, U. C., Lawrence, M., Galy-Lacaux, C., Rast, S., Shindell, D., Stevenson, D., Van Noije, T., Atherton, C., Bell, N., Bergman, D., Butler, T., Cofala, J., Collins, B., Doherty, R., Ellingsen, K., Galloway, J., Gauss, M., Montanaro, V., Müller, J.-F., Pitari, G., Rodriguez, J., Sanderson, M., Solmon, F., Strahan, S., Schultz, M., Sudo, K., Szopa, S., and Wild, O.: Nitrogen and sulfur deposition on regional and global scales: A multimodel evaluation, *Global Biogeochem. Cy.*, 20, GB4003, doi:10.1029/2005GB002672, 2006.

Eder, B. and Yu, S.: A performance evaluation of the 2004 release of Models-3 CMAQ, *Atmos. Environ.*, 40, 4811–4824, 2006.

Erismann, J. W., Vanelzakker, B. G., Mennen, M. G., Hogenkamp, H., Zwart, E., Van den Beld, L., Romer, F. G., Bobbink, R., Heil, G., Raessen, M., Duyzer, J. H., Verhage, H., Wyers, G. P., Otjes, R. P., and Möls, J. J.: The Elspeetsche Veldexperiment on surface exchange of trace gases: summary of results, *Atmos. Environ.*, 28, 487–496, 1994a.

Erismann, J. W., Mennen, M., Hogenkamp, J., Kemkers, E., Godhart, D., van Pul, A., Draaijers, G., Duyzer, J., and Wyers, P.: Dry deposition monitoring of SO₂, NH₃ and NO₂ over a coniferous forest, edited by: Borrell, P. M., Borrell, P., Cvitas, T., and Seiler, W., *Proceedings of EUROTRAC Symposium '94*, The Hague, The Netherlands, 655–659, 1994b.

Fenn, R. W., Gerber, H. E., and Wasshuasen, D.: Measurements of the sulphur and ammonium

**Particulate
ammonium modelling
for North America
using AURAMS**P. A. Makar et al.

[Title Page](#)[Abstract](#)[Introduction](#)[Conclusions](#)[References](#)[Tables](#)[Figures](#)[⏪](#)[⏩](#)[◀](#)[▶](#)[Back](#)[Close](#)[Full Screen / Esc](#)[Printer-friendly Version](#)[Interactive Discussion](#)

- component of the arctic aerosol of the Greenland icecap, *J. Atmos. Sci.*, 20, 466–468, 1963.
- Fenn, M. E., Jovan, S., Yuan, F., Geiser, L., Meixner, T., and Gimeno, B. S.: Empirical and simulated critical loads for nitrogen deposition in California mixed conifer forests, *Environ. Pollut.*, 155(3), 492–511, 2008.
- 5 Fowler, D., Cape, J. N., Coyle, M., Smith, R. I., Hjellbrekke, A.-G., Simpson, D., Derwent, R. G., and Johnson, C. E.: Modelling photochemical oxidant formation, transport, deposition and exposure of terrestrial ecosystems, *Environ. Pollut.*, 100, 43–55, 1998.
- Fung, C. S., Misra, P. K., Bloxam, R., and Wong, S.: A numerical experiment on the relative importance of H_2O_2 and O_3 in aqueous conversion of SO_2 to SO_4 , *Atmos. Environ.*, 25(A), 411–423, 1991.
- 10 Gilliland, A. B., Appel, K. W., Pinder, R. W., and Dennis, R. L.: Seasonal NH_3 emissions for the continental United States: inverse model estimation and evaluation, *Atmos. Environ.*, 40, 4986–4998, 2006.
- Gong, W., Dastoor, A. P., Bouchet, V. S., Gong, S., Makar, P. A., Moran, M. D., Pabla, B., Ménard, S., Crevier, L.-P., Cousineau, S., and Venkatesh, S.: Cloud processing of gases and aerosols in a regional air quality model (AURAMS), *Atmos. Res.*, 82, 248–275, 2006.
- Gordon, R. J. and Bryan, R. J.: Ammonium nitrate in airborne particles in Los Angeles, *Environ. Sci. Technol.*, 7, 645–647, 1973.
- 15 Hall, J., Hornung, M., Kennedy, F., Langan, S., Reynolds, B., and Aherne, J.: Investigating the uncertainties in the simple mass balance equation for acidity critical loads for terrestrial ecosystems, *Water Air Soil Poll.*, 1, 43–56, 2001.
- Heard, M. J. and Wiffen, R. D.: Electron microscopy of natural aerosols and the identification of particulate ammonium sulphate, *Atmos. Environ.*, 3, 337–340, 1969.
- Herrmann, H., Ervens, B., Jacobi, H.-W., Wolke, R., Nowack, P., and Zellner, R. CAPRAM2.3: A Chemical Aqueous Phase Radical Chemistry for Tropospheric Chemistry, *J. Atmos. Chem.*, 25 36, 231–284, 2000.
- Herrmann, H., Tilgner, A., Barzagli, P., Majdik, Z., Gligorovski, S., Poulain, L., and Monod, A.: Towards a more detailed description of tropospheric aqueous phase organic chemistry: CAPRAM 3.0., *Atmos. Environ.*, 39, 4351–4363, 2005.
- 30 Houyoux, M. R., Vukovich, J. M., Coats Jr., C. J., and Wheeler, N. J. M.: Emission inventory development and processing for the Seasonal Model for Regional Air Quality (SMRAQ) project, *J. Geophys. Res.*, 105, 9079–9090, 2000.
- Jeffries, D. S. and Ouimet, R.: Critical loads: are they being exceeded?, Chapter 8 of Cana-

- dian Acid Deposition Science Assessment 2004, Environment Canada, 4905 Dufferin Street, Downsview, Canada, 440 pp., 2004.
- Jeffries, D. S., Lam, D. C. L., Moran, M. D., and Wong, I.: The effect of SO₂ emission controls on critical load exceedances for lakes in southeastern Canada, *Water Sci. Tech.*, 39, 165–171, 1999.
- Junge, C. E. and Ryan, T. G.: Study of the SO₂ oxidation in solution and its role in atmospheric chemistry, *Q. J. Roy. Meteorol. Soc.*, 84, 46–55, 1958.
- Kusik, C. L. and Meissner, H. P.: Electrolyte activity coefficients in inorganic processing, *A. I. Ch. E. Symposium*, 173, 14–20, 1978.
- Logan, J. A.: An analysis of ozonesonde data for the troposphere: Recommendations for testing 3-D models, and development of a gridded climatology for tropospheric ozone, *J. Geophys. Res.*, 104, 16115–16149, 1998.
- Luo, C., Zender, C. S., Bian, H., and Metzger, S.: Role of ammonia chemistry and coarse mode aerosols in global climatological inorganic aerosol distributions, *Atmos. Environ.*, 41, 2510–2533, 2007.
- MacDonald, A. M., Anlauf, K. G., Leaitch, W. R., and Liu, P. S.: Multi-year Chemistry of Particles and Selected Trace Gases at the Whistler High Elevation Site, *EOS Trans. AGU*, 87(52), Fall Meet., Suppl., Abstract A53b-0179, 2006.
- Makar, P. A., Bouchet, V. S., and Nenes, A.: Inorganic chemistry calculations using HETV – a vectorized solver for the SO₄²⁻-NO₃⁻-NH₄⁺ system based on the ISORROPIA algorithms, *Atmos. Environ.*, 37, 2279–2294, 2003.
- Mathur, R. and Dennis, R. L.: Seasonal and annual modeling of reduced nitrogen compounds over the eastern United States: Emissions, ambient levels, and deposition amounts, *J. Geophys. Res.-Atmos.*, 108, ACH 22-1–ACH 22-19, 2003.
- McNulty, S. G., Cohen, E. C., Moore Myers, J. A., Sullivan, T. J., and Li, H.: Estimates of critical acid loads and exceedances for forest soils across the conterminous United States, *Environ. Pollut.*, 149, 281–292, 2007.
- Moran, M. D., Zheng, Q., Samaali, M., Narayan, J., Pavlovic, R., Cousineau, S., Bouchet, V. S., Sassi, M., Makar, P. A., Gong, W., Gong, S., Stroud, C., and Duhamel, A.: Comprehensive surface-based performance evaluation of a size-and composition-resolved regional particulate-matter model for a one-year simulation, *Proc. 29th NATO/SPS ITM on Air Pollution Modelling and Its Application*, Aveiro, Portugal, 24–28 September, 9 pp., in: *Air Pollution Modeling and its Application XIX*, 2008, edited by: Borrego, C. and Miranda, A. I., Springer,

**Particulate
ammonium modelling
for North America
using AURAMS**P. A. Makar et al.

[Title Page](#)[Abstract](#)[Introduction](#)[Conclusions](#)[References](#)[Tables](#)[Figures](#)[⏪](#)[⏩](#)[◀](#)[▶](#)[Back](#)[Close](#)[Full Screen / Esc](#)[Printer-friendly Version](#)[Interactive Discussion](#)

**Particulate
ammonium modelling
for North America
using AURAMS**

P. A. Makar et al.

[Title Page](#)[Abstract](#)[Introduction](#)[Conclusions](#)[References](#)[Tables](#)[Figures](#)[⏪](#)[⏩](#)[◀](#)[▶](#)[Back](#)[Close](#)[Full Screen / Esc](#)[Printer-friendly Version](#)[Interactive Discussion](#)

Dordrecht, The Netherlands, 434–442, 2007.

Moran, M. D., Zheng, Q., Pavlovic, R., Cousineau, S., Bouchet, V. S., Sassi, M., Makar, P. A., Gong, W., and Stroud, C.: Predicted acid deposition critical-load exceedances across Canada from a one-year simulation with a regional particulate-matter model, Proc. 15th Joint AMS/A&WMA Conf. on Applications of Air Pollution Meteorology, 21–24 January, New Orleans, American Meteorological Society, Boston, 20 pp., online available at: <http://ams.confex.com/ams/pdfpapers/132916.pdf>, 2008.

Neiryneck, J., Kowalski, A. S., Carrara, A., and Ceulemans, R.: Driving forces for ammonia fluxes over mixed forest subjected to high deposition loads, *Atmos. Environ.*, 39, 5013–5024, 2005.

Phillips, S. B., Aneja, V. P., Kang, D., and Arya, S. P.: Modelling and analysis of the atmospheric nitrogen deposition in North Carolina, *International Journal of Global Environmental Issues*, 6, 231–252, 2006.

Quan, J. and Zhang, X.: Assessing the role of ammonia in sulfur transformation and deposition in China, *Atmos. Res.*, 88, 78–88, 2008.

Robbins, R. C. and Cadle, R. D.: Kinetics of the reaction between gaseous ammonia and sulfuric acid droplets in an aerosol, *J. Phys. Chem.*, 62, 469–471, 1958.

Schwarze, P. E., Orevik, J., Lag, M., Refsnes, M., Nafstad, P., Hetland, R. B., and Dybing, E.: Particulate matter properties and health effects: Consistency of epidemiological and toxicological studies, *Hum. Exp. Toxicol.*, 25, 559–579, 2006.

Scire, J. S., Lurmann, F. W., Karamchandani, P., Venkatram, A., Yamartino, R., Young, J., and Pleim, J., ADOM/TADAP Model Development Program, Volume 9: User's Guide, Environmental Research and Technology, Inc., Newbury Park, California, USA, 1986.

Seinfeld, J. H. and Pandis, S. N.: *Atmospheric chemistry and physics: from air pollution to climate change*, John Wiley and Sons, Inc., New York, USA, 1326 pp., 1998.

Spranger, T., Hettelingh, J.-P., Slootweg, J., and Posch, M.: Modelling and mapping long-term risks due to reactive nitrogen effects: An overview of LRTAP convention activities, *Environ. Pollut.*, 154, 482–487, 2008.

Spurny, K. and Heard, M. J.: Discussions: Electron microscopy of natural aerosols and the identification of particulate ammonium sulphate, *Atmos. Environ.*, 3, p. 483, 1969.

Stelson, A. W., Friedlander, S. K., and Seinfeld, J. H.: A note on the equilibrium relationship between ammonia and nitric acid and particulate ammonium nitrate, *Atmos. Environ.*, 13, 369–371, 1979.

Stilg, M.: *World-wide limits for toxic and hazardous chemicals*, Noyes Publications, N.J.,

**Particulate
ammonium modelling
for North America
using AURAMS**

P. A. Makar et al.

[Title Page](#)[Abstract](#)[Introduction](#)[Conclusions](#)[References](#)[Tables](#)[Figures](#)[⏪](#)[⏩](#)[◀](#)[▶](#)[Back](#)[Close](#)[Full Screen / Esc](#)[Printer-friendly Version](#)[Interactive Discussion](#)

792 pp., 1994.

Stockwell, W. R. and Calvert, J. G.: The mechanism of the HO-SO₂ reaction, *Atmos. Environ.*, 17, 2231–2235, 1983.

Sutton, M. A., Asman, W. A. H., and Schjorring, J. K.: Dry deposition of reduced nitrogen, *Tellus*, 46, 255–273, 1994.

Tanner, R. L.: An ambient experimental study of phase equilibrium in the atmospheric system: aerosol H⁺, NH₄⁺, SO₄²⁻, NO₃⁻, NH₃(g), HNO₃(g), *Atmos. Environ.*, 16, 2935–2942, 1983.

Van Hove, L. W. A., Adema, E. H., Vredenberg, W. H., and Pieters, G. A.: A study of the adsorption of NH₃ and SO₂ on leaf surfaces, *Atmos. Environ.*, 23, 1479–1486, 1989.

Venkatram, A., Karamchandani, P. K.: Testing a comprehensive acid deposition model, *Atmos. Environ.*, 22, 737–747, 1988.

Wang, J., Deeter, M. N., Gille, J. C., and Bailey, P. L.: Retrieval of tropospheric carbon monoxide profiles from MOPITT: Algorithm description and retrieval simulation, *Proceedings of SPIE – The International Society for Optical Engineering*, 3756, 437–446, 1999.

Wang, Z., Xie, F., Sakurai, T., Ueda, H., Han, Z., Carmichael, G. R., Streets, D., Engardt, M., Holloway, T., Hayami, H., Kajino, M., Thongboonchoo, N., Bennet, C., Park, S. U., Fung, C., Chang, A., Sartelet, K., and Amann, M.: MICS-Asia II: Model inter-comparison and evaluation of acid deposition, *Atmos. Environ.*, 42, 3528–3542, 2008.

Ying, Q. and Kleeman, M. J.: Source contributions to the regional distribution of secondary particulate matter in California, *Atmos. Environ.*, 40, 736–752, 2006.

Yu, S., Dennis, R., Roselle, S., Nenes, A., Walker, J., Eder, B., Schere, K., Swall, J., and Rorbarge, W.: An assessment of the ability of three-dimensional air quality models with current thermodynamic equilibrium models to predict aerosol NO₃⁻, *J. Geophys. Res.*, 110, 22 pp., doi:10.1029/2004JD004718, 2005.

Zhang, L., Gong, S., Padro, J., and Barrie, L.: A size-segregated particle dry deposition scheme for an atmospheric aerosol module, *Atmos. Environ.*, 35, 549–560, 2001.

Zhang, L., Moran, M. D., Makar, P. A., Brook, J. R., and Gong, S.: Modelling gaseous dry deposition in AURAMS: a unified regional air-quality modelling system, *Atmos. Environ.*, 36, 537–560, 2002.

Table 1. Metrics for chemical evaluation of model responses to NH₃ emission changes.

Metric	Formula	Significance
Particle Neutralization Ratio	$\frac{(\rho - \text{NH}_4)}{2(\rho - \text{SO}_4) + (\rho - \text{NO}_3)}$	Ratio of total ammonium charge to the net sulphate and nitrate charge (each particle species variable is the sum over all particle sizes). Values of 1 indicate that the particles are NH ₃ -saturated, so that significant NH ₃ reductions may be required to reduce particulate mass. Regions with values less than unity are more NH ₃ -limited; smaller reductions in NH ₃ may result in significant reductions in particulate mass.
Total ammonia to sulphate mole ratio	$\frac{(\text{NH}_3(\text{g})) + (\rho - \text{NH}_4)}{(\rho - \text{SO}_4)}$	Mole ratio of ammonia gas + particle ammonia to particle sulphate. This defines the chemical regime: values less than unity denote acidic conditions (e.g., ammonium bisulphate, sulphuric acid present in the particles); values between 1.0 and 2.0 denote intermediate acidity (ammonium bisulphate, letovicite, ammonium sulphate present), and values greater than 2 indicate less acidic particles (ammonium sulphate, ammonium nitrate may be present in the particles). Note that a decrease in the value of the ratio does not necessarily imply a significant change in the particle composition, if the initial and final values of the ratio are both high.
Gas-phase fraction ammonia mass	$\frac{(\text{NH}_3)}{(\text{PM}_{2.5} - \text{NH}_4) + (\text{NH}_3)}$	Relative mass of NH ₃ in the gas phase to total ammonia + ammonium mass. Changes in this parameter indicate a change in the mass partitioning of ambient NH ₃ in response to changes in NH ₃ emissions.
PM _{2.5} Ammonium + Nitrate to total PM _{2.5} mass ratio	$\frac{(\text{PM}_{2.5} - \text{NH}_4) + (\text{PM}_{2.5} - \text{NO}_3)}{(\text{PM}_{2.5})}$	Fraction of fine particle mass that is directly ammonia-sensitive. A diagnostic of the direct impact of emissions reductions.

Particulate ammonium modelling for North America using AURAMS

P. A. Makar et al.

Title Page

Abstract

Introduction

Conclusions

References

Tables

Figures

⏪

⏩

◀

▶

Back

Close

Full Screen / Esc

Printer-friendly Version

Interactive Discussion

Table 2. Statistical measures of model performance. N is the number of paired observed-model values, \bar{O} is the mean observed value, \bar{M} is the mean model value.

Statistical Measure	Description	Formula
R	Pearson Correlation Coefficient	$R = \frac{N \sum_{i=1}^N (O_i \times M_i) - \sum_{i=1}^N (M_i) \sum_{i=1}^N (O_i)}{\sqrt{N \sum_{i=1}^N (M_i \times M_i) - \sum_{i=1}^N (M_i) \times \sum_{i=1}^N (M_i)} \sqrt{N \sum_{i=1}^N (O_i \times O_i) - \sum_{i=1}^N (O_i) \times \sum_{i=1}^N (O_i)}}$
b	Slope of observations vs. model best-fit line	$b = \frac{\sum_{i=1}^N [(O_i - \bar{O})(M_i - \bar{M})]}{\sum_{i=1}^N [(O_i - \bar{O})^2]}$
a	Intercept of observations vs. model best-fit line	$a = \bar{M} - b \times \bar{O}$
MB	Mean bias	$MB = \frac{1}{N} \sum_{i=1}^N (M_i - O_i)$
RMSE	Root Mean Square Error	$RMSE = \sqrt{\frac{1}{N} \sum_{i=1}^N (M_i - O_i)^2}$
NMB	Normalized Mean Bias	$NMB = \frac{\sum_{i=1}^N (M_i - O_i)}{\sum_{i=1}^N O_i} \times 100$
NME	Normalized Mean Error	$NME = \frac{\sum_{i=1}^N M_i - O_i }{\sum_{i=1}^N O_i} \times 100$

Particulate ammonium modelling for North America using AURAMS

P. A. Makar et al.

Title Page

Abstract

Introduction

Conclusions

References

Tables

Figures

◀

▶

◀

▶

Back

Close

Full Screen / Esc

Printer-friendly Version

Interactive Discussion

Particulate ammonium modelling for North America using AURAMS

P. A. Makar et al.

Table 3. Annual statistics for selected AURAMS gas- and particle-phase species. Statistical metrics are defined in Table 2.

Statistic	SO ₂ (ppbv)	HNO ₃ (ppbv)	PM _{2.5} ($\mu\text{g m}^{-3}$, STP)	PM _{2.5} -SO ₄ ($\mu\text{g m}^{-3}$, STP)	PM _{2.5} -NO ₃ ($\mu\text{g m}^{-3}$, STP)	PM _{2.5} -NH ₄ ($\mu\text{g m}^{-3}$, STP)
Networks	a,d,e,g	d,e	a,b,c,f,g,h	c,f,h	c,f,h	c,h
<i>N</i>	451	86	845	265	254	141
\overline{O}	3.32	0.53	11.33	2.77	1.28	1.53
\overline{M}	3.55	0.66	7.87	2.26	1.05	1.25
<i>a</i>	1.01	0.08	-0.74	-0.64	0.12	0.23
<i>b</i>	0.77	1.10	0.76	1.04	0.73	0.66
<i>R</i>	0.56	0.81	0.65	0.92	0.77	0.76
MB	0.23	0.13	-3.46	-0.51	-0.23	-0.29
RMSE	2.88	0.28	5.00	0.95	1.01	0.54
NMB (%)	7.0	25.2	-30.5	-18.5	-17.9	-18.7
NME (%)	51.7	38.3	36.8	27.3	43.5	27.2

Networks: a: AQS-continuous; b: AQS-filter; c: AQS-STN; d: CAPMoN; e: CASTNet; f: IMPROVE; g: NAPS-continuous; h: NAPS-filter.

Title Page

Abstract

Introduction

Conclusions

References

Tables

Figures

⏪

⏩

◀

▶

Back

Close

Full Screen / Esc

Printer-friendly Version

Interactive Discussion

Particulate ammonium modelling for North America using AURAMS

P. A. Makar et al.

Table 4. Annual statistics for several AURAMS wet deposited species. Measurements were obtained from five Canadian precipitation-chemistry networks (CAPMoN, BCPCSN, NBPMN, PQMPA, REPQ) and one US network (NADP).

Statistic	SO ₄ ²⁻ conc. in precip. (mg SO ₄ /L)	NO ₃ ⁻ conc. in precip. (mg NO ₃ /L)	NH ₄ ⁺ conc. in precip. (mg NH ₄ /L)	SO ₄ ²⁻ wet dep. (kg SO ₄ /ha/y)	NO ₃ ⁻ wet dep. (kg NO ₃ /ha/y)	NH ₄ ⁺ wet dep. (kg NH ₄ /ha/y)
<i>N</i>	277	270	271	277	270	271
\bar{O}	1.08	1.11	0.31	10.1	9.39	2.39
\bar{M}	0.96	0.94	0.21	9.54	8.30	1.81
<i>a</i>	-0.03	0.202	0.021	0.449	1.46	0.11
<i>b</i>	0.91	0.67	0.60	0.90	0.73	0.71
<i>R</i>	0.81	0.61	0.76	0.84	0.71	0.78
MB	-0.12	-0.17	-0.10	-0.58	-1.09	-0.58
RMSE	0.37	0.50	0.16	3.94	4.24	1.07
NMB (%)	-11.4	-15.0	-33.1	-5.8	-11.6	-24.1
NME (%)	24.8	33.4	36.2	28.3	33.7	33.9

Title Page

Abstract

Introduction

Conclusions

References

Tables

Figures

◀

▶

◀

▶

Back

Close

Full Screen / Esc

Printer-friendly Version

Interactive Discussion

Particulate ammonium modelling for North America using AURAMS

P. A. Makar et al.

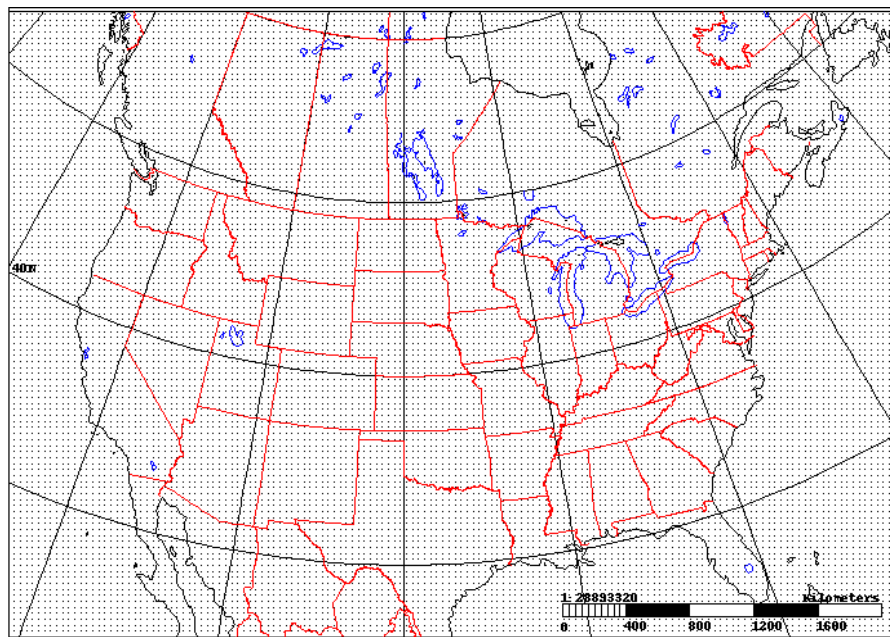


Fig. 1. AURAMS CTM North American 150×106 42-km domain.

[Title Page](#)[Abstract](#)[Introduction](#)[Conclusions](#)[References](#)[Tables](#)[Figures](#)[⏪](#)[⏩](#)[◀](#)[▶](#)[Back](#)[Close](#)[Full Screen / Esc](#)[Printer-friendly Version](#)[Interactive Discussion](#)

Particulate ammonium modelling for North America using AURAMSP. A. Makar et al.

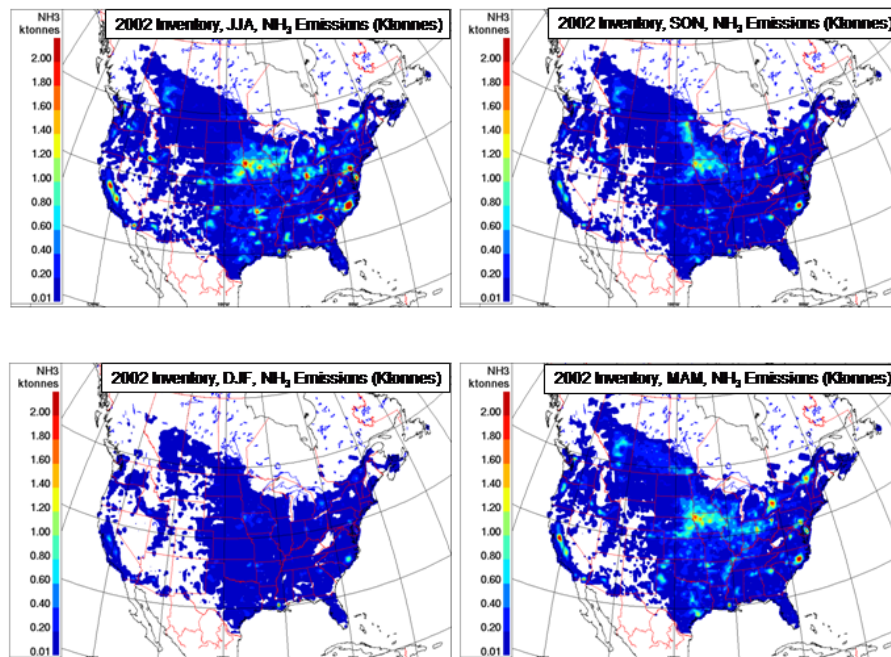


Fig. 2. Ammonia emissions (kilotonnes) in each season. Upper left: June-July-August; upper right: September-October-November; lower left: December-January-February; lower right: March-April-May.

[Title Page](#)[Abstract](#)[Introduction](#)[Conclusions](#)[References](#)[Tables](#)[Figures](#)[⏪](#)[⏩](#)[◀](#)[▶](#)[Back](#)[Close](#)[Full Screen / Esc](#)[Printer-friendly Version](#)[Interactive Discussion](#)

Particulate ammonium modelling for North America using AURAMSP. A. Makar et al.

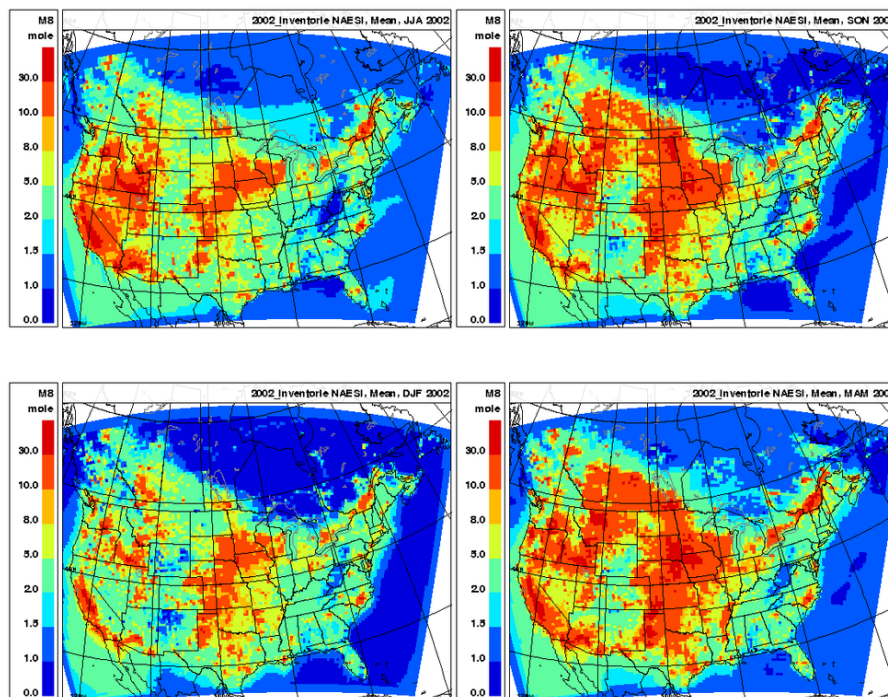


Fig. 3. Seasonal total NH_3 to sulphate mole ratio for base-case simulation: summer – upper left; fall – upper right; winter – lower left; spring – lower right.

[Title Page](#)[Abstract](#)[Introduction](#)[Conclusions](#)[References](#)[Tables](#)[Figures](#)[⏪](#)[⏩](#)[◀](#)[▶](#)[Back](#)[Close](#)[Full Screen / Esc](#)[Printer-friendly Version](#)[Interactive Discussion](#)

Particulate ammonium modelling for North America using AURAMS

P. A. Makar et al.

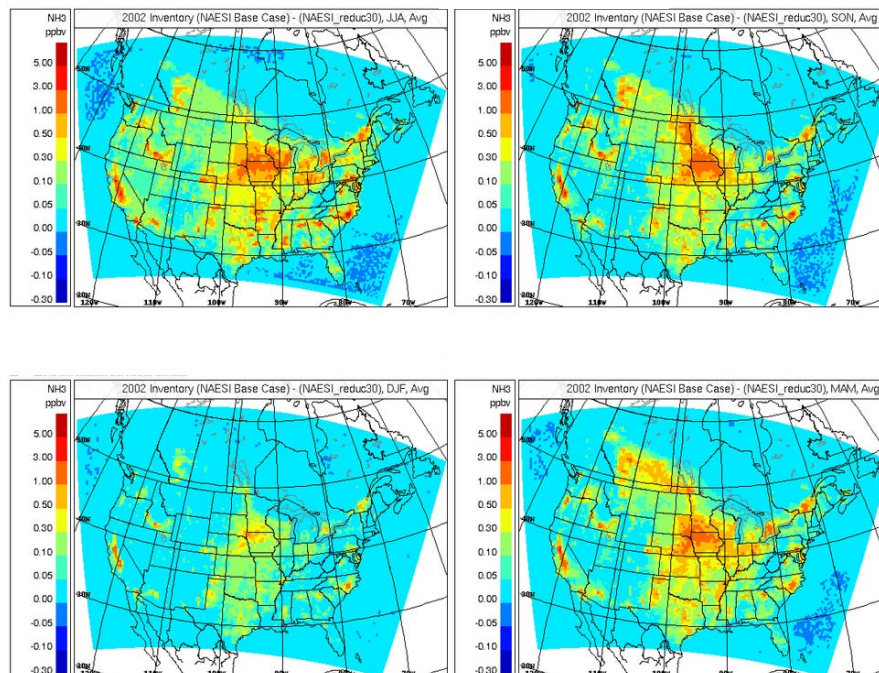


Fig. 4. Seasonal average change in NH_3 concentration, ppbv, associated with a 30% reduction in agricultural NH_3 emissions. Panels arranged as in Fig. 2.

[Title Page](#)[Abstract](#)[Introduction](#)[Conclusions](#)[References](#)[Tables](#)[Figures](#)[◀](#)[▶](#)[◀](#)[▶](#)[Back](#)[Close](#)[Full Screen / Esc](#)[Printer-friendly Version](#)[Interactive Discussion](#)

Particulate ammonium modelling for North America using AURAMS

P. A. Makar et al.

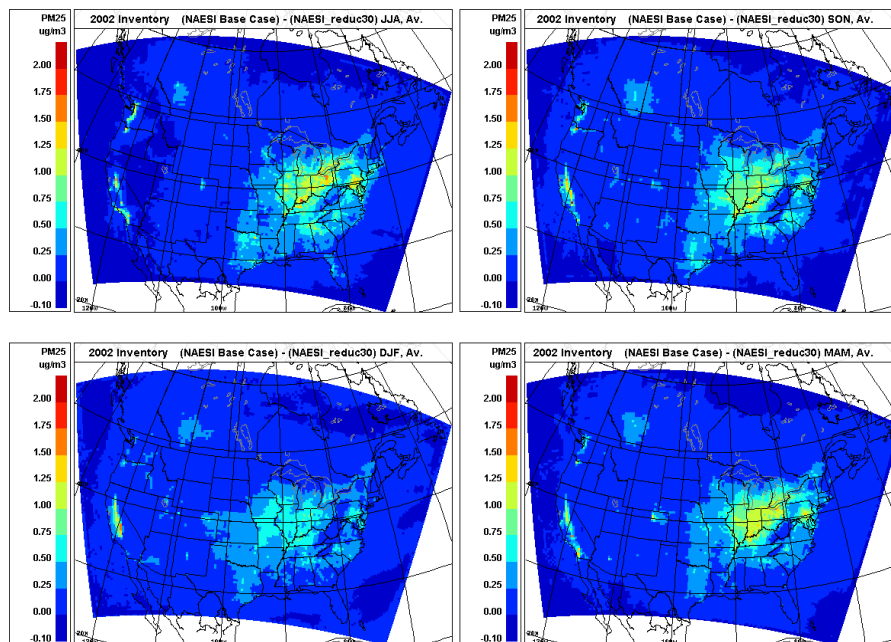


Fig. 5. Seasonal average change in $\text{PM}_{2.5}$ mass, $\mu\text{g m}^{-3}$, associated with a 30% reduction in agricultural NH_3 emissions. Panels arranged as in Fig. 2.

Title Page

Abstract

Introduction

Conclusions

References

Tables

Figures

⏪

⏩

◀

▶

Back

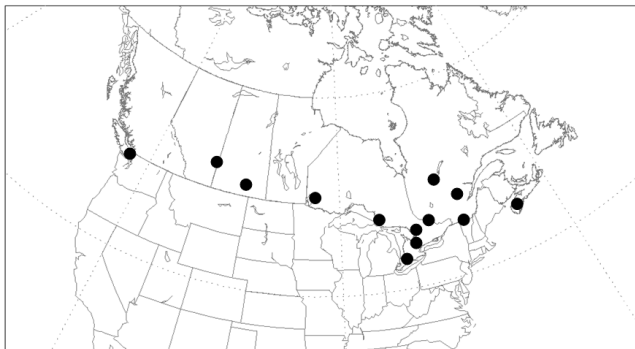
Close

Full Screen / Esc

Printer-friendly Version

Interactive Discussion

CAPMoN Filter Chemistry Monitors in 2002



CASTNet Filter Chemistry Monitors in 2002

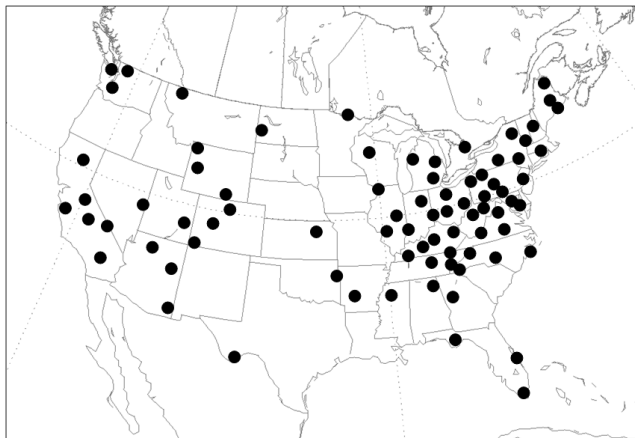


Fig. 6. Locations of sites used in analysis of episodic nature of ammonia emissions reductions: **(a)** Canadian CAPMoN sites; **(b)** US CASTNet sites.

Title Page

Abstract

Introduction

Conclusions

References

Tables

Figures

◀

▶

◀

▶

Back

Close

Full Screen / Esc

Printer-friendly Version

Interactive Discussion

Particulate ammonium modelling for North America using AURAMS

P. A. Makar et al.

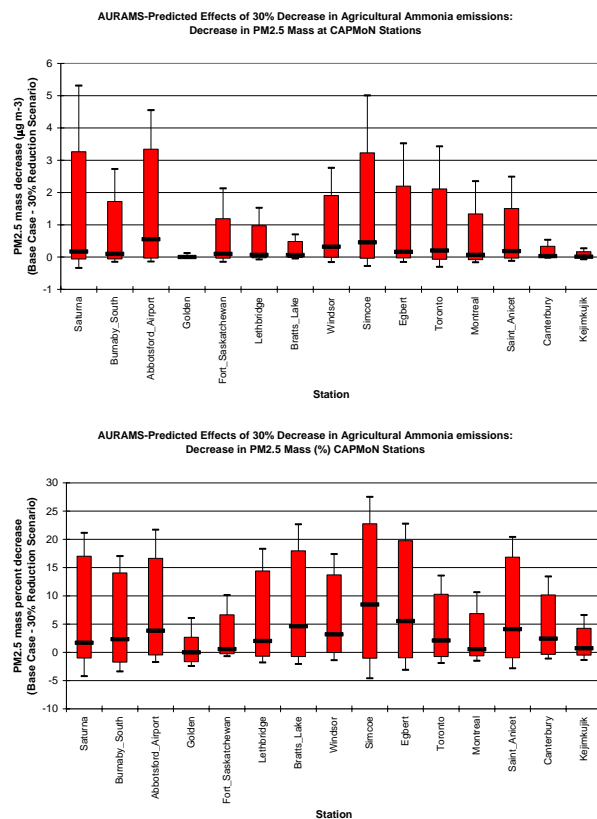


Fig. 7. AURAMS-predicted annual frequency distributions of the decrease in hourly PM_{2.5} concentrations associated with a 30% decrease in NH₃ emissions at CAPMoN stations (numbered sites from Fig. 6a): **(a)** expressed in mass units; **(b)** expressed as percentage difference relative to the base case. Median: solid horizontal bar; 5 and 95 percentiles: limits of red vertical bar; 2 and 98 percentiles: thin horizontal bars.

Title Page

Abstract

Introduction

Conclusions

References

Tables

Figures

◀

▶

◀

▶

Back

Close

Full Screen / Esc

Printer-friendly Version

Interactive Discussion

Particulate ammonium modelling for North America using AURAMS

P. A. Makar et al.

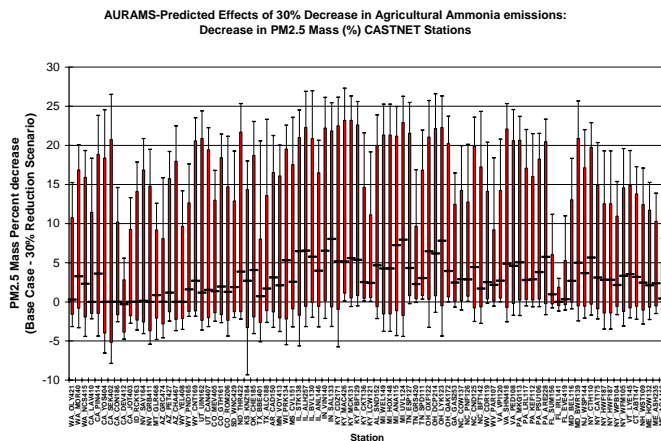
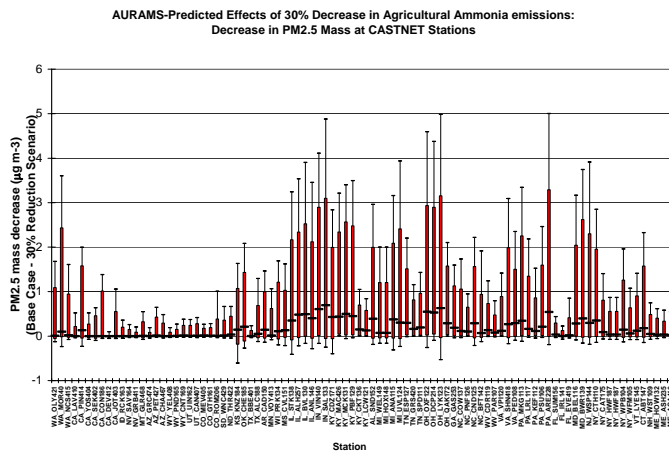


Fig. 8. Same as Fig. 6 but for CASTNet station sites shown in Fig. 5b.

Title Page	
Abstract	Introduction
Conclusions	References
Tables	Figures
◀	▶
◀	▶
Back	Close
Full Screen / Esc	
Printer-friendly Version	
Interactive Discussion	

Particulate ammonium modelling for North America using AURAMSP. A. Makar et al.

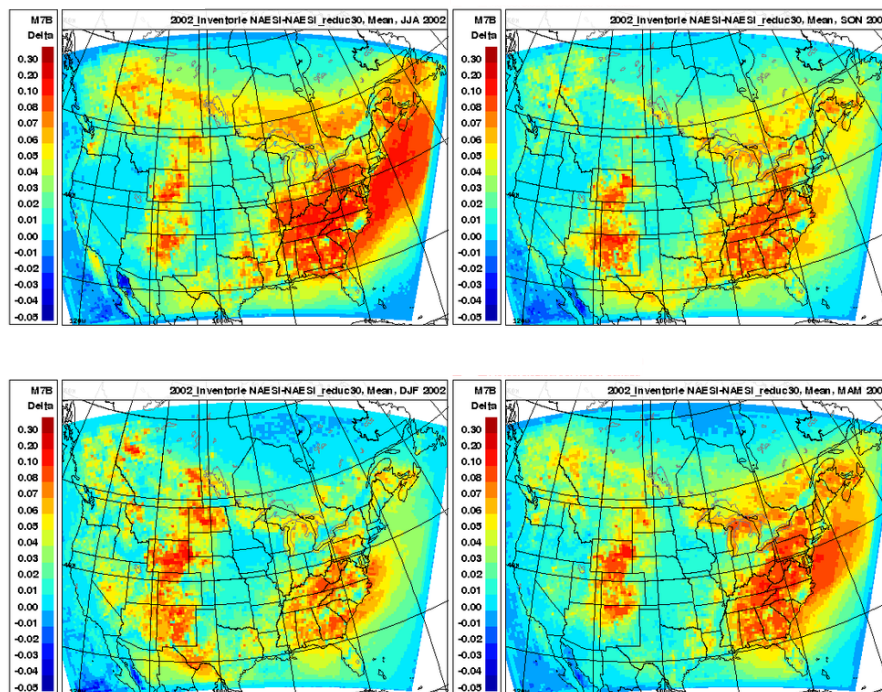


Fig. 9. Change in particle neutralization ratio due to 30% reduction in NH_3 emissions. Positive regions indicate increased particle acidity relative to the base case. Panels arranged as in Fig. 2.

[Title Page](#)[Abstract](#)[Introduction](#)[Conclusions](#)[References](#)[Tables](#)[Figures](#)[◀](#)[▶](#)[◀](#)[▶](#)[Back](#)[Close](#)[Full Screen / Esc](#)[Printer-friendly Version](#)[Interactive Discussion](#)

**Particulate
ammonium modelling
for North America
using AURAMS**P. A. Makar et al.

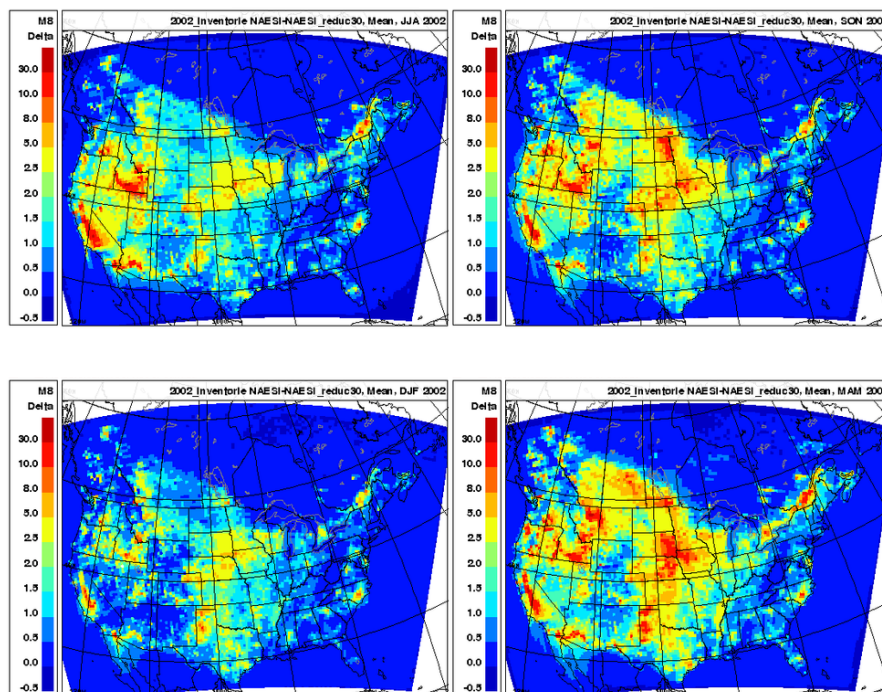


Fig. 10. Change in total ammonia to sulphate mole ratio due to 30% reduction in NH_3 emissions. Positive regions indicate decreases in the ratio (more acidic chemical regimes) relative to the base case. Panels arranged as in Fig. 2.

[Title Page](#)[Abstract](#)[Introduction](#)[Conclusions](#)[References](#)[Tables](#)[Figures](#)[⏪](#)[⏩](#)[◀](#)[▶](#)[Back](#)[Close](#)[Full Screen / Esc](#)[Printer-friendly Version](#)[Interactive Discussion](#)

Particulate ammonium modelling for North America using AURAMSP. A. Makar et al.

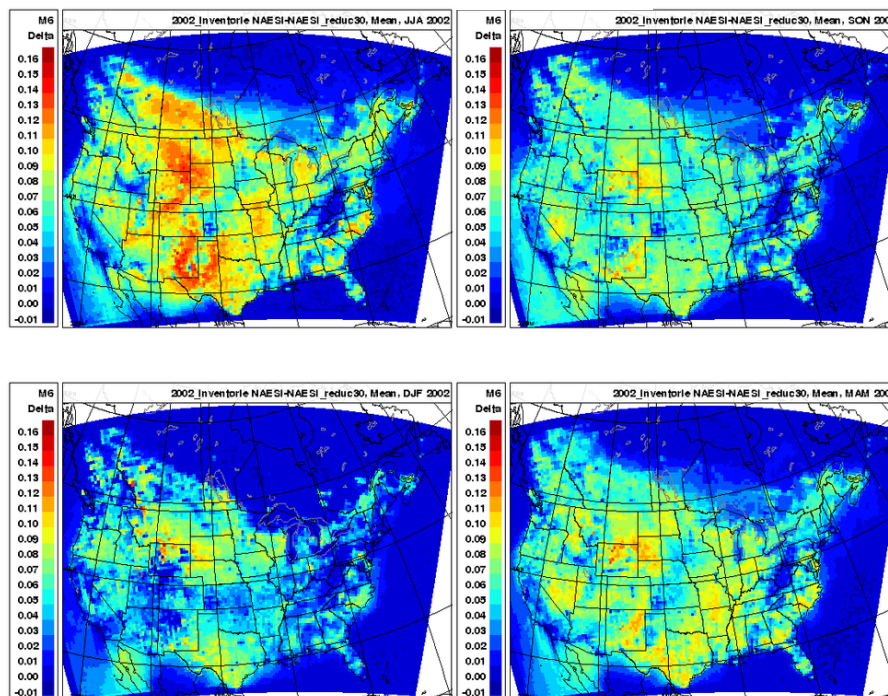


Fig. 11. Change in gas-phase NH_3 mass fraction due to 30% reduction in NH_3 emissions. Positive regions indicate decreases in mass fraction (i.e., proportionately more ammonium in the particle phase) relative to the base case. Panels arranged as in Fig. 2.

[Title Page](#)[Abstract](#)[Introduction](#)[Conclusions](#)[References](#)[Tables](#)[Figures](#)[⏪](#)[⏩](#)[◀](#)[▶](#)[Back](#)[Close](#)[Full Screen / Esc](#)[Printer-friendly Version](#)[Interactive Discussion](#)

Particulate ammonium modelling for North America using AURAMSP. A. Makar et al.

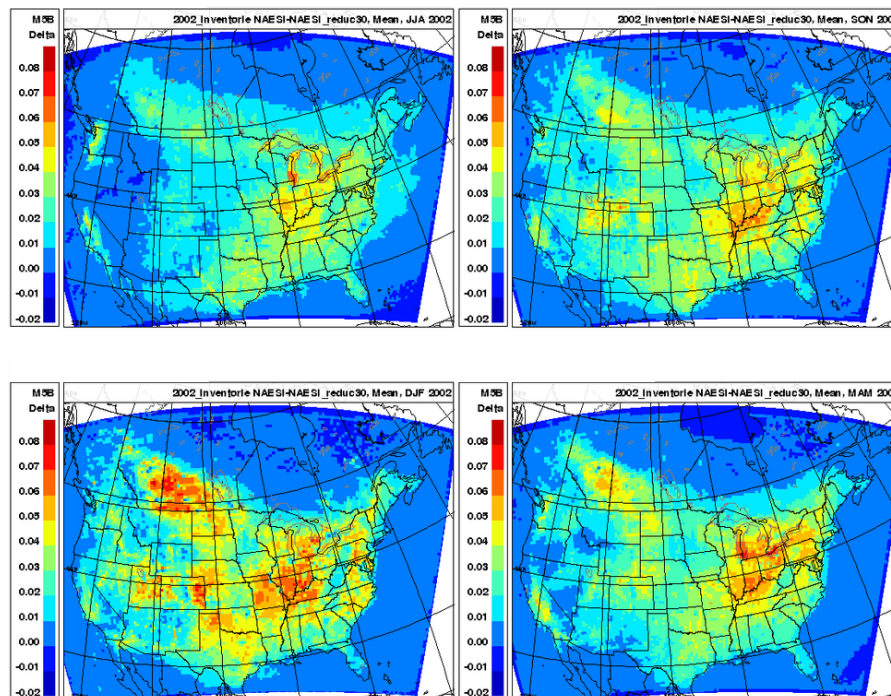


Fig. 12. Change in fraction of ammonium + nitrate mass in $PM_{2.5}$ relative to the total $PM_{2.5}$ mass. Positive regions indicate decreases in ammonium and nitrate mass fraction (i.e., particles composed of proportionately less ammonium and nitrate) relative to the base case. Panels arranged as in Fig. 2.

[Title Page](#)[Abstract](#)[Introduction](#)[Conclusions](#)[References](#)[Tables](#)[Figures](#)[⏪](#)[⏩](#)[◀](#)[▶](#)[Back](#)[Close](#)[Full Screen / Esc](#)[Printer-friendly Version](#)[Interactive Discussion](#)

Particulate ammonium modelling for North America using AURAMS

P. A. Makar et al.

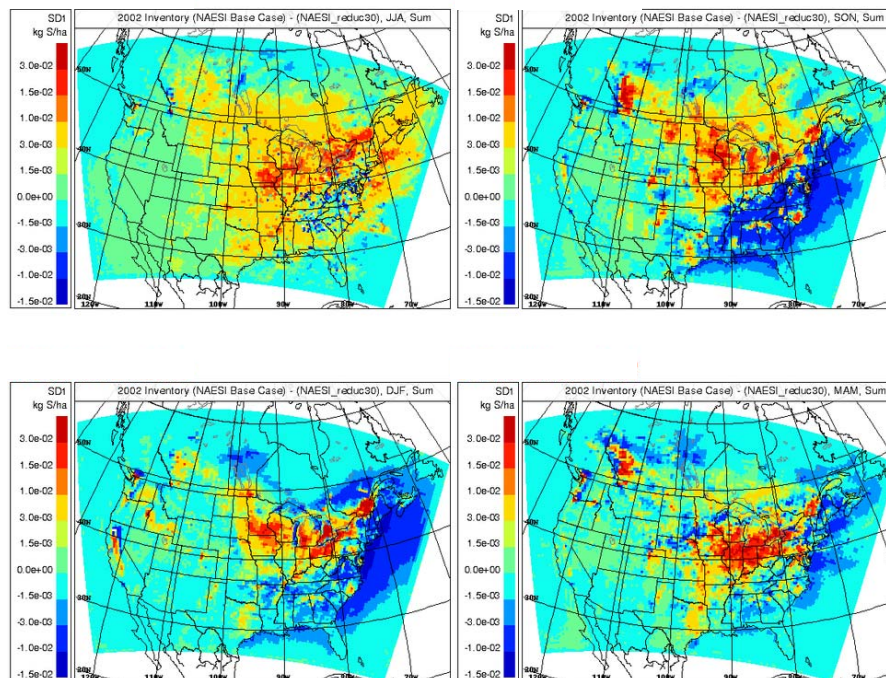


Fig. 13. Change in total – sulphur total deposition (kg S/ha/season) due to 30% reduction in NH_3 emissions. Positive values (green to red colours) indicate decreases in sulphur deposition resulting from decreasing NH_3 emissions; negative values (blue) indicate increases in sulphur deposition resulting from decreasing NH_3 emissions. Panels arranged as in Fig. 2.

Title Page

Abstract

Introduction

Conclusions

References

Tables

Figures

◀

▶

◀

▶

Back

Close

Full Screen / Esc

Printer-friendly Version

Interactive Discussion

Particulate ammonium modelling for North America using AURAMS

P. A. Makar et al.

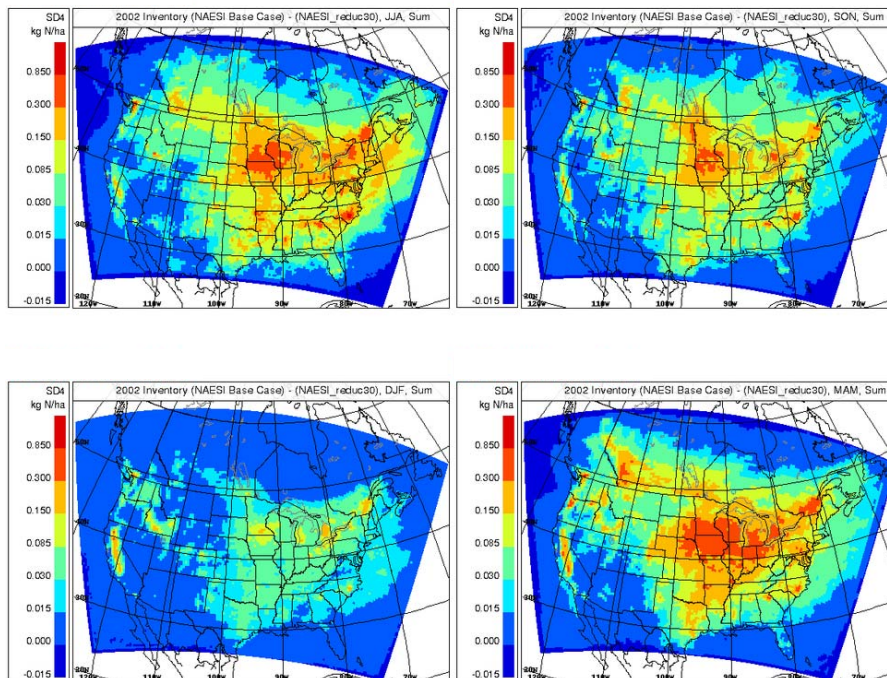


Fig. 14. Same as Fig. 13 but for total-nitrogen total deposition (kg N/ha/season).

[Title Page](#)[Abstract](#)[Introduction](#)[Conclusions](#)[References](#)[Tables](#)[Figures](#)[◀](#)[▶](#)[◀](#)[▶](#)[Back](#)[Close](#)[Full Screen / Esc](#)[Printer-friendly Version](#)[Interactive Discussion](#)

Particulate ammonium modelling for North America using AURAMS

P. A. Makar et al.

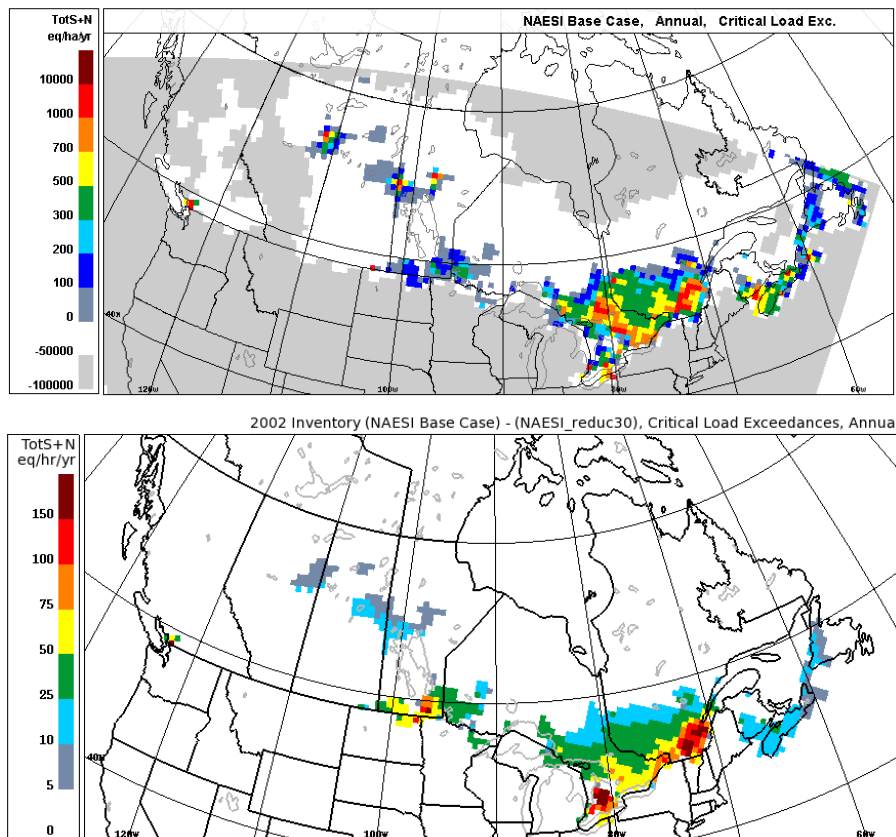


Fig. 15. AURAMS-predicted Canadian (S+N) critical-load exceedances for 2002: (top) NAESI base case; and (bottom) base case – 30% NH_3 emissions reduction scenario. Gray areas in the top panel indicate areas for which critical-load values were not available. Positive values in the bottom panel indicate areas where the critical load exceedance has decreased in response to decreasing NH_3 emissions.

[Title Page](#)[Abstract](#)[Introduction](#)[Conclusions](#)[References](#)[Tables](#)[Figures](#)[◀](#)[▶](#)[◀](#)[▶](#)[Back](#)[Close](#)[Full Screen / Esc](#)[Printer-friendly Version](#)[Interactive Discussion](#)

Particulate ammonium modelling for North America using AURAMS

P. A. Makar et al.

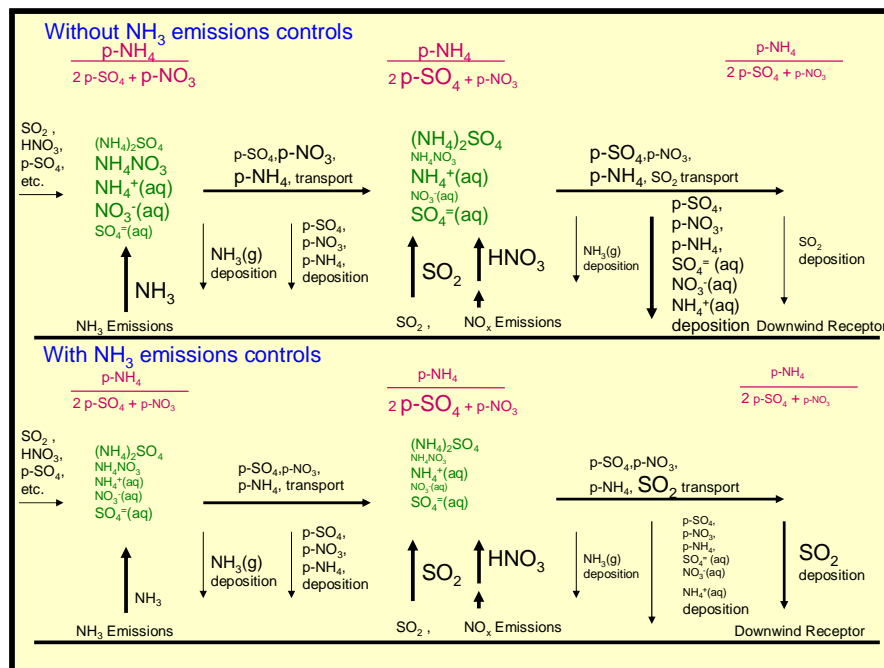


Fig. 16. Conceptual model of NH₃ emissions, reaction and transport: (top) without NH₃ emissions controls; (bottom) with NH₃ emissions controls.

Title Page

Abstract

Introduction

Conclusions

References

Tables

Figures

⏪

⏩

⏪

⏩

Back

Close

Full Screen / Esc

Printer-friendly Version

Interactive Discussion

Particulate ammonium modelling for North America using AURAMS

P. A. Makar et al.

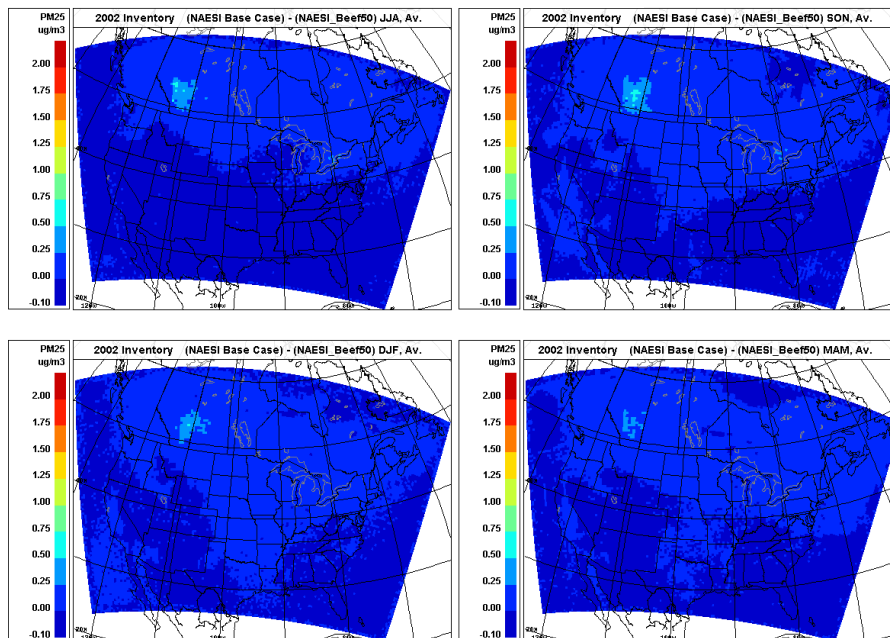


Fig. 17. Seasonal average change in PM_{2.5} mass ($\mu\text{g m}^{-3}$) associated with a 50% reduction in Canadian beef-cattle emissions. Panels arranged as in Fig. 2.

Title Page

Abstract

Introduction

Conclusions

References

Tables

Figures

⏪

⏩

◀

▶

Back

Close

Full Screen / Esc

Printer-friendly Version

Interactive Discussion